

DTIC FILE COPY Technical Report  
771

# Adaptive-Reference Near- and Far-Echo Cancellation in the Presence of Frequency Offset

AD-A182 212

T.F. Quatieri  
G.C. O'Leary

22 May 1987

**Lincoln Laboratory**

MASSACHUSETTS INSTITUTE OF TECHNOLOGY

LEXINGTON, MASSACHUSETTS



Prepared for the Department of Defense  
under Electronic Systems Division Contract F19628-85-C-0002.

Approved for public release; distribution unlimited.

DTIC  
ELECTE  
JUL 15 1987  
S E D

The work reported in this document was performed at Lincoln Laboratory, a center for research operated by Massachusetts Institute of Technology. This work was sponsored by the Department of Defense under Air Force Contract F19628-85-C-0002.

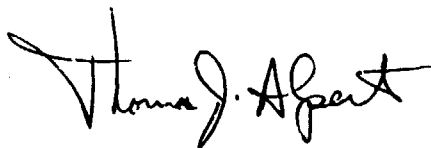
This report may be reproduced to satisfy needs of U.S. Government agencies.

The views and conclusions contained in this document are those of the contractor and should not be interpreted as necessarily representing the official policies, either expressed or implied, of the United States Government.

The ESD Public Affairs Office has reviewed this report, and it is releasable to the National Technical Information Service, where it will be available to the general public, including foreign nationals.

This technical report has been reviewed and is approved for publication.

FOR THE COMMANDER



Thomas J. Alpert, Major, USAF  
Chief, ESD Lincoln Laboratory Project Office

Non-Lincoln Recipients

**PLEASE DO NOT RETURN**

Permission is given to destroy this document  
when it is no longer needed.

**MASSACHUSETTS INSTITUTE OF TECHNOLOGY  
LINCOLN LABORATORY**

**ADAPTIVE-REFERENCE NEAR- AND FAR-ECHO  
CANCELLATION IN THE PRESENCE OF FREQUENCY OFFSET**

*T.F. QUATIERI*

*G.C. O'LEARY*

*Group 24*

**TECHNICAL REPORT 771**

**22 MAY 1987**

**Approved for public release; distribution unlimited.**

**LEXINGTON**

**MASSACHUSETTS**

87-7-14-032

## ABSTRACT

This report presents the results of a study of the applicability of various echo-cancelling techniques to the problem of improving the transmission of data over voiceband telephone channels. The principal result of the study is a design for a novel echo-cancelling configuration which permits the cancellation of a far-echo component containing a frequency offset. The modem design is based on a combined adaptive-reference echo canceller and adaptive-channel equalizer. The adaptive-reference algorithm has the advantage that interference to the echo canceller caused by the far-end signal can be eliminated by subtracting an estimate of the far-end signal based on receiver decisions. This technique is extended to provide a new approach for full-duplex far-echo cancellation in which the far echo can be cancelled in spite of carrier frequency offset. To estimate the frequency offset, the system uses a separate receiver structure for the far echo which provides equalization of the far-echo channel and tracks the frequency offset in the far echo. The feasibility of the echo-cancelling algorithms is demonstrated by computer simulation with realistic channel distortions and with 4800 b/s data transmission, at which rate frequency offset in the far echo becomes important. The design requirements for a modem implementing this algorithm are examined briefly.

Accession For	
NTIS GRA&I	<input checked="" type="checkbox"/>
DTIC TAB	<input type="checkbox"/>
Unannounced	<input type="checkbox"/>
Justification	
By	
Distribution/	
Availability Codes	
Dist	Avail and/or Special
A-1	



## TABLE OF CONTENTS

Abstract	iii
List of Illustrations	vii
List of Tables	viii
 1. INTRODUCTION	 1
2. ADAPTIVE-REFERENCE ECHO CANCELLATION	3
2.1 Channel Models	3
2.2 Adaptive-Reference Near-Echo Cancellation	3
2.3 The Effect of Frequency Offset	11
3. ADAPTIVE-REFERENCE ECHO CANCELLATION WITH FREQUENCY OFFSET ESTIMATION	13
3.1 Cancellation with a Known Offset	13
3.2 Adaptive-Reference Near-Echo Cancellation with Unknown Frequency Offset in the Far-End Signal	16
3.3 Adaptive-Reference Far-Echo Cancellation with Frequency Offset in the Far Echo	19
3.4 The Composite System	19
4. EVALUATION OF THE NEAR- AND FAR-ECHO-CANCELLING MODEM ALGORITHM AT 4800 b/s	25
4.1 Frequency Offset in the Far-Echo Channel	26
4.2 Frequency Offset in the Far Echo and Far-End Signal	28
4.3 Other Channel Distortions	28
5. AN RLS ADAPTIVE-REFERENCE ECHO-CANCELLING MODEM	35
6. IMPLEMENTATION	37
7. SUMMARY AND DISCUSSION	41

## LIST OF ILLUSTRATIONS

Figure No.		Page
1-1	Typical Dialed Telephone Connection	1
2-1	Adaptive-Reference Near-Echo Canceller	4
2-2	Performance of Echo-Cancelling Modem Algorithm With and Without Adaptive Reference at 4800 bs	10
2-3	Effect of Convergence Gain on AREC Response with Far-Echo Frequency Offset	12
3-1	Adaptive Structure for Replicating a Passband Modem Signal with a Known Frequency Offset	14
3-2	Canceller with Far-Echo Cancellation and Known Frequency Offsets in Far Echo and Far-End Signal	15
3-3	Canceller with Correction for Frequency Offset in Far-End Signal	17
3-4	Canceller with Correction for Far-Echo Frequency Offset	20
3-5	Canceller with Correction for Far-Echo and Far-Signal Frequency Offset	21
3-6	Preamble Timing Scenario for Near/Far-Echo-Cancelling Modem Algorithm	23
4-1	Performance of Far-Echo-Cancelling Modem Algorithm (No Near Echo)	26
4-2	Error Residuals of Modem Algorithm with Frequency Offset in Far Echo. (a) Residuals with Respect to Far Signal at Far-Signal Receiver, (b) Residuals with Respect to Far Echo Receiver, (c) Signal-to-Echo Residual at Equalizer Input.	27
4-3	Response of Modem Algorithm with Frequency Offset in Far Signal and Far-Echo Paths. (a) Far-End-Signal Frequency-Offset, (b) Far-Echo Frequency Offset, (c) $S/E_0$ .	29
4-4	Performance of Complete Modem Design with Phase Hits. (a) $S/E_0$ , (b) Accumulated Receiver Errors, (c) Far-End-Signal Frequency-Offset Estimate, (d) Far-Echo Frequency Offset.	30
4-5	Performance of Complete Modem with Phase Hits and Impulse Noise. (a) $S/E_0$ , (b) Accumulated Receiver Errors, (c) Far-End-Signal Frequency-Offset Estimate, (d) Far-Echo Frequency-Offset Estimate.	32

<b>Figure No.</b>		<b>Page</b>
4-6	Performance of Complete Modem Design with Phase Hits and Impulse Noise (Near-Echo-to-Signal Ratio = 40 dB). (a) $S/E_n$ , (b) Accumulated Receiver Errors, (c) Far-End-Signal Frequency-Offset Estimate, (d) Far-Echo Frequency-Offset Estimate.	33
5-1	Comparison of LMS and RLS Near-Echo Adaptive-Reference Cancellers	36
6-1	DSP32 Configuration of the Modem Design	38

## LIST OF TABLES

<b>Table No.</b>		<b>Page</b>
I	Measured and Predicted S/E (dB) for Echo-Cancelling Modem Algorithm With and Without Adaptive Reference at 4800 b/s	10
II	Design Specifications for Near/Far-Echo-Cancelling Modem Algorithm	25
III	Computational Requirements for Modem Algorithm	37

# ADAPTIVE-REFERENCE NEAR- AND FAR-ECHO CANCELLATION IN THE PRESENCE OF FREQUENCY OFFSET

## 1. INTRODUCTION

Adaptive echo cancellers used in high-speed ( $\geq 4800$  b/s) full-duplex voiceband data transmission must suppress both the near and far echoes which occur on the telephone connection.<sup>1,2</sup> A simplified view of a typical dialed telephone connection in Figure 1-1 shows the various hybrids in the network. Echoes are generated by imperfect impedance matching at these hybrids. Both the near and far echo suffer from linear dispersion in the channel, but the far echo also contains other effects such as carrier-frequency offset, abrupt carrier-phase changes (phase hits), and phase jitter.<sup>1,3,4</sup> In addition to such anomalies, the adaptive echo cancellers must contend with interference from the wanted far-end signal ("double-talk"), and interference of the echoes themselves (e.g., the far echo as an interference to the near echo). Current echo cancellers deal with these sources of interference by a two-stage process. The adaptive filters are initially trained in a half-duplex mode with convergence gains set to permit rapid adaptation to the channel. During actual operation the gains are set to allow only very slow adaptation, thus averaging out the effect of the interfering signals.<sup>5</sup>

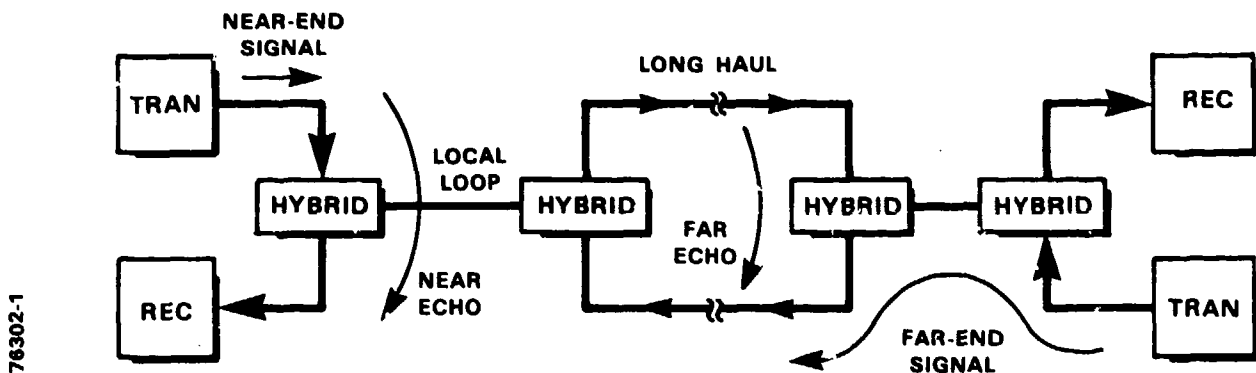


Figure 1-1. Typical dialed telephone connection.

In this report we demonstrate the design of a full-duplex echo-cancelling voiceband modem which is capable of continuous and rapid adaptation. This system generalizes the adaptive-reference echo canceller (AREC) proposed by Falconer,<sup>6</sup> by cancelling far echo with carrier-frequency offset. In the AREC approach to echo cancellation the interference from the far-end signal is eliminated by subtracting a far-end-signal estimate derived from receiver decisions.

We begin by describing an adaptive-reference near-echo canceller combined with an adaptive filter which compensates for the channel distortions introduced into the far-end signal and which also acts as a matched filter for this signal. With the adaptive-reference feature, the near-echo



canceller can run with much faster response time than the conventional canceller and, in fact, the canceller can achieve initial convergence in the full-duplex mode. The adaptive-reference near-echo canceller is further extended by introducing a frequency tracking loop used to compensate for the carrier-frequency offset in the far-end signal.

Elimination of the effects of the far echo is more difficult. The far echo is typically smaller than the desired far-end signal, but not so small that it does not affect the receiver's ability to demodulate the signal. The far echo actually becomes one of the limiting factors in receiver performance at 4800 b/s and above. The elimination of the far echo is further complicated by the fact that it has traversed the channel twice and has been subjected to the linear distortions and frequency offset uncertainties of each trip. Only a slight amount of frequency offset in the far echo can result in a considerable loss of suppression with traditional echo cancellers.<sup>1</sup>

We generalize here the AREC receiver structure to eliminate the far-echo interference. The basic technique is first to enhance the visibility of the far echo by subtracting estimates of the two major interfering signals, the near echo and the far signal. A separate adaptive-receiver structure is then used to demodulate the enhanced far-echo signal and make an estimate of its frequency offset. Once this offset is determined, adaptive cancellation of the far echo is possible in the same way that the near echo is cancelled. The feasibility of the complete system is demonstrated under a wide range of realistic operating conditions which include frequency offset, white and impulse noise, and phase hits in both the far-end signal and far echo.

The adaptive structures in our adaptive-reference near- and far-echo-cancelling modem design are based on the least-mean-squares (LMS) update procedure,<sup>10</sup> thus following the approach of Falconer.<sup>6</sup> An alternative method, proposed for improving the canceller's tracking ability by faster adaptation, employs a recursive least-squares (RLS)<sup>11</sup> version of the LMS adaptation process. Here the LMS adaptive canceller and simulator are replaced by their RLS counterparts. We will observe, however, that since in our configuration the input to these filters is white (i.e., driven by uncorrelated data symbols), the RLS adaptation gives no advantage over the LMS, neither in initial convergence time nor in frequency offset tracking. The RLS adaptation may be useful, however, in channel equalization, especially at very high data rates.

The report is organized as follows. In Section 2 we review channel models for the near and far echo and far-end signal and conventional methods of echo cancellation. Then the adaptive-reference echo canceller is described. The performance degradation produced by frequency offset in the far echo and far-end signal is illustrated. In Section 3 we present the new adaptive-reference near- and far-echo-cancelling modem algorithm. This is done first with a near- and far-echo canceller with a known frequency offset. The problem of frequency offset is then addressed, first in the far-end signal and then in the far echo. In Section 4 we compare the frequency-offset-tracking capability of the new canceller with the basic adaptive-reference canceller, and evaluate its performance and demonstrate its robustness. Then, in Section 5 we explore the RLS counterpart to the LMS adaptation procedure, and in Section 6 we investigate the LMS algorithm's computational requirements and present one implementation based on the recent signal processing chip, AT&Ts WF DSP32 (Reference 18). Finally, in Section 7 we summarize the report and consider remaining questions and future directions.

## 2. ADAPTIVE-REFERENCE ECHO CANCELLATION

In this section we first review the sources of echo and the notion of echo cancellation. The adaptive-reference near-echo canceller is then described and its ability to accommodate far echo and far-end-signal frequency offset is demonstrated to be inadequate.

### 2.1 Channel Models

The transmitted signal consists of the sum of complex symbols  $I_k$  shaped by a window function and modulated on a carrier. The resulting transmitted signal is given by

$$s_t(nT) = \text{Re} \left\{ \sum_k I_k p[(n - kL) T] \exp[j\omega_c nT] \right\} \quad (2-1)$$

where  $p(nT)$  is the value of the shaping pulse at time  $nT$  (where  $T$  is the sampling interval),  $1/L$  is the symbol (or baud) rate, and  $\omega_c/2\pi$  is the carrier frequency. When  $s_t(nT)$  is passed through a linear channel and returns as an echo, it appears in the receiver in the form

$$s_r(nT) = \text{Re} \left\{ \sum_k I_k g[(n - kL) T] \exp[j\omega_c nT + \phi(nT)] \right\} \quad (2-2)$$

where  $g(nT)$  is the composite baseband impulse response consisting of the convolution of the transmit pulse and echo-channel impulse response. The phase shift,  $\phi(nT)$ , added by the channel, is generally time-varying of the form

$$\phi(nT) = \omega_o nT + \phi_o(nT) \quad (2-3)$$

where the first term represents the phase change due to a frequency offset  $\omega_o$  and the residual  $\phi_o(nT)$  may include constant phase offset, phase hits and phase jitter (typically, quasi-periodic). Generally, the near echo suffers from only linear channel distortion introduced by the local hybrid, while the far echo can suffer from all distortions given by Equations (2-2) and (2-3). Likewise, the desired far-end signal can also suffer from these distortions. The complete received signal can be written as

$$r(nT) = s_N(nT) + s_F(nT) + f(nT) + w(nT) \quad (2-4)$$

where  $s_N(nT)$  and  $s_F(nT)$  denote the near and far echoes, respectively,  $f(nT)$  denotes the far-end signal, and  $w(nT)$  is additive noise with both white and impulse-like components.<sup>3</sup>

### 2.2 Adaptive-Reference Near-Echo Cancellation

In the conventional approach to echo cancellation<sup>2,7,8,9</sup> the near-end signal is passed through an adaptive filter which attempts to emulate the echo formation process. The filter output, which is an echo estimate, is subtracted from the received signal before the receiver performs demodulation and channel equalization. In order to simulate linear channel distortion, each canceller typically employs a finite-impulse response filter whose taps are estimated adaptively. A steepest-descent approach is often used to minimize the average squared error between the echo estimates

and the received signal, leading to the least-mean-squares (LMS) update for estimating the canceller coefficients.<sup>10</sup> Other faster adaptation procedures, such as recursive least squares estimation, have also been applied.<sup>11</sup> Since the adaptation in these algorithms depends on the measured difference between the actual echo and the echo estimate, the far-end signal in Equation (2-4) introduces a large noise source to adaptation. In addition, the far echo acts as a noise source to the near-echo canceller and vice versa. The goal of adaptive-reference cancellation is to prevent each signal from acting as interference in the various adaptation processes.

In adaptive-reference echo cancellation,<sup>6</sup> the far-end signal is estimated and subtracted from the echo residual before it has a chance to corrupt the canceller adaptation. A discrete time representation of an adaptive-reference near-echo-cancelling modem algorithm is illustrated in Figure 2-1. This system combines the adaptive-reference technique<sup>6</sup> with an adaptive far-end-channel equalizer. All the adaptive filters used in the system use complex tap coefficients, thus producing a complex baseband representation of the echo which is then converted back to a passband signal for cancellation.

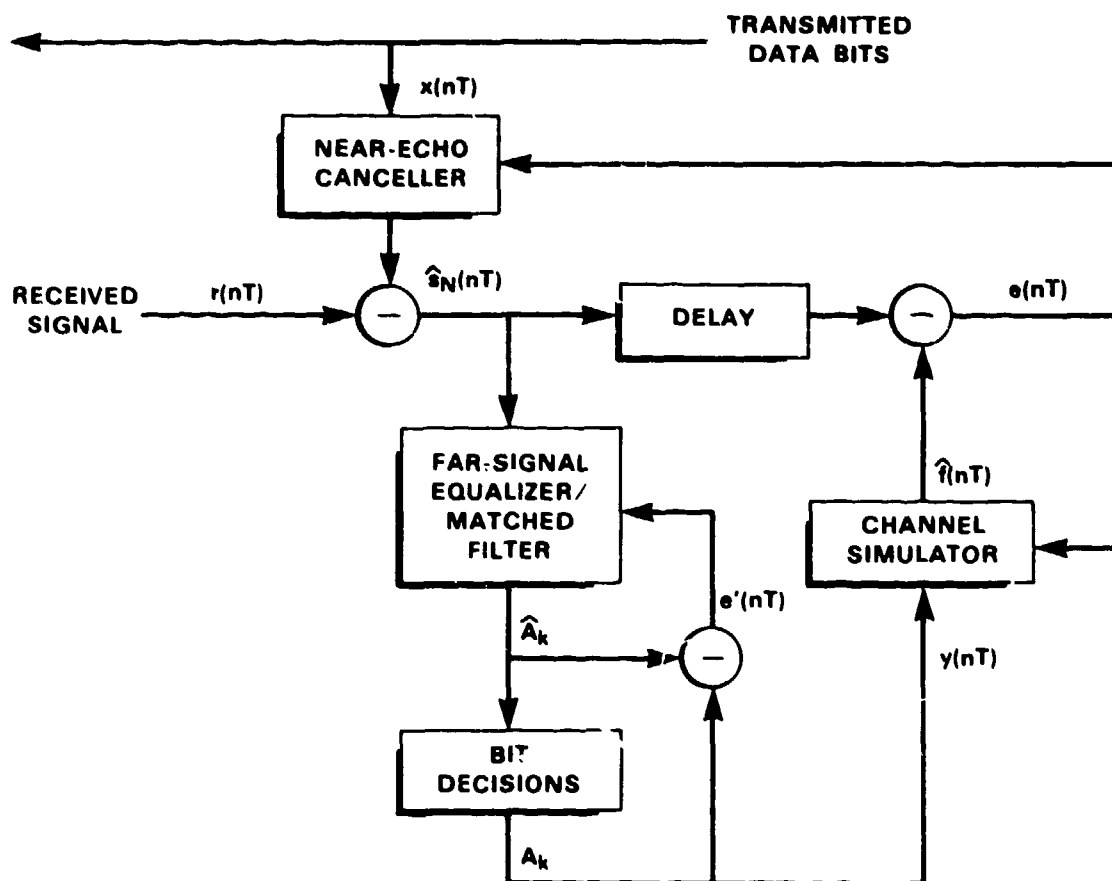


Figure 2-1. Adaptive-reference near-echo canceller.

The receiver of Figure 2-1 employs three adaptive filters. The first filter combines the functions of a channel equalizer with that of a matched filter. It provides the input to the decision-making process. The second filter is the echo canceller. It takes the transmitted symbols as its input and tries to simulate the echo. The simulated echo is subtracted from the received signal to improve the performance of the matched filter. This difference signal is also used to control the adaptation of the echo canceller. Since this difference also contains the far-end signal, the signal-to-interference ratio at this point is poor. The third adaptive filter, the channel simulator, is used to improve this ratio. This filter generates an estimate of the received far-end signal based on the bit decisions made at the receiver. The adaptation capability of this filter allows it to simulate the linear distortions in the far-end signal. Both the echo canceller and the channel simulator adapt jointly from the same error signal, using the iterative LMS technique to minimize the residual error. This error will be a minimum when the echo canceller is exactly modelling the echo channel and the channel simulator is modelling the channel from the far-end modem.

In this realization both the echo canceller and the channel simulator use tapped delay lines with complex coefficients. They generate a complex baseband representation of the signal. The baseband representation is mixed back to passband and the real part is used to form the real error signal,  $e(nT)$ . Let  $\underline{a}(nT)$  and  $\underline{b}(nT)$  represent the complex tap coefficient vectors of these filters, and let  $\underline{x}(nT)$  and  $\underline{y}(nT)$  represent the complex data-symbol vectors in the echo canceller and channel simulator, respectively, at time  $nT$ . The coefficient adaptation is based on a least-mean-squares (LMS) update<sup>2,6,10</sup> derived by minimizing, with respect to  $\underline{a}(nT)$  and  $\underline{b}(nT)$ , the mean-squared residual error  $e(nT)$  given by

$$e(nT) = r(nT) - [\hat{s}_N(nT) + \hat{f}(nT)] \quad (2-5a)$$

with the near-echo estimate  $\hat{s}_N(nT)$

$$\hat{s}_N(nT) = \text{Re}\{\underline{x}^t(nT) \underline{a}(nT) \exp[j\omega_c nT]\} \quad (2-5b)$$

with the far-end signal estimate  $\hat{f}(nT)$

$$\hat{f}(nT) = \text{Re}\{\underline{y}^t(nT) \underline{b}(nT) \exp[j\omega_c nT]\} \quad (2-5c)$$

and where, without loss of generality, we have assumed that the delay in Figure 2-1 equals zero. This delay element is required to account for the processing time through the equalizer and simulator. We then solve for the unknown near-echo-canceller and channel-simulator coefficients by using the method of steepest descent<sup>10</sup> to solve the problem

$$\text{minimize } E[e^2(nT)] \quad (2-6a)$$

with respect to  $\underline{a}(nT)$  and  $\underline{b}(nT)$  where "E" denotes expected value. For the real signal  $e(nT)$  the problem (2-6a) is equivalent to the problem

$$\text{minimize } E\{[\epsilon(nT) + \epsilon^*(nT)]^2\} \quad (2-6b)$$

with respect to  $\underline{a}(nT)$  and  $\underline{b}(nT)$  where "\*" denotes complex conjugate, and where we have defined the complex error

$$\epsilon(nT) = r(nT) - \underline{x}^t(nT) \underline{a}(nT) \exp[j\omega_c nT] - \underline{y}^t(nT) \underline{b}(nT) \exp[j\omega_c nT]. \quad (2-6c)$$

From Equation (2-6), it is straightforward to show that the gradients required in the method of steepest descent are given by

$$\nabla E[e^2(nT)] = -2E\{e(nT) \underline{x}^*(nT) \exp[-j\omega_c nT]\} \quad (2-7a)$$

with respect to  $\underline{a}(nT)$  and

$$\nabla E[e^2(nT)] = -2E\{e(nT) \underline{y}^*(nT) \exp[-j\omega_c nT]\} \quad (2-7b)$$

with respect to  $\underline{b}(nT)$ . Since the expected values in Equations (2-7a) and (2-7b) are not generally available, we use the "instantaneous gradient"<sup>10</sup> as an estimate:

$$\nabla E[e^2(nT)] \approx -2e(nT) \underline{x}^*(nT) \exp[-j\omega_c nT] \quad (2-7c)$$

with respect to  $\underline{a}(nT)$  and

$$\nabla E[e^2(nT)] \approx -2e(nT) \underline{y}^*(nT) \exp[-j\omega_c nT] \quad (2-7d)$$

with respect to  $\underline{b}(nT)$ . The optimization thus yields the iterative LMS update equations given by

$$\underline{a}[(n+1)T] = \underline{a}(nT) + \mu_c \underline{x}^*(nT) e(nT) \exp[-j\omega_c nT] \quad (2-8a)$$

and

$$\underline{b}[(n+1)T] = \underline{b}(nT) + \mu_s \underline{y}^*(nT) e(nT) \exp[-j\omega_c nT] \quad (2-8b)$$

where  $\mu_c$  and  $\mu_s$  are the convergence factors for the echo canceller and channel simulator, respectively. We can interpret the mixing operation in Equation (2-8) as a translation of the passband error residual  $e(nT)$  to baseband where the adaptive filters are operating. For simplicity, these mixing operations, as well as the translation and real component operations at the output of the canceller and simulator tapped delay lines, have been included in their associated modules of Figure 2-1.

The equalizer/matched filter also consists of complex coefficients and complex adaptation. The adaptation for the equalizer coefficients  $\underline{g}(nT)$  is derived by minimizing, with respect to  $\underline{g}(nT)$ , the mean-squared value of  $e'(nT)$  evaluated at baud intervals at time  $nT = kLT$ . This error is the difference between the far-end complex symbols,  $A_k$ , and their estimates  $\hat{A}_k$  as depicted in Figure 2-1. The LMS update based on the optimization of the equalizer coefficients, which takes place at the baud rate, is given by

$$\underline{g}[(k+1)LT] = \underline{g}(kLT) + \mu_e \underline{z}^*(kLT) e'(kLT) \exp[-j\omega_c kLT] \quad (2-9a)$$

where  $\mu_e$  is the convergence gain factor and  $\underline{z}(kLT)$  is the demodulated (echo-compensated) input vector, with

$$\underline{z}(nT) = [r(nT) - \hat{s}(nT)] \exp[-j\omega_c nT] \quad (2-9b)$$

where the complex exponential in (2-9b) translates to baseband the input to the equalizer tapped delay line. Both mixing operations in (2-9) have been assumed included in the equalizer module of Figure 2-1. The values  $A_k$  used to compute the error for the equalizer/matched filter are the bit decisions for the far-end signal. We assume in this analysis that the decisions are correct. We can guarantee this during the transmission of a known preamble. During data transmission the occurrence of occasional decision errors does not seriously affect performance.

Falconer<sup>6</sup> has provided an analysis of an adaptive-reference canceller with real coefficients and a bipolar (+1 or -1) symbol train  $A_k$ . Extending Falconer's approach we can obtain an expression for the average power of the residual echo in the echo-cancelling modem structure of Figure 2-1. As in Reference 6, we assume that the data vectors  $\underline{x}(nT)$  and  $\underline{y}(nT)$  in the canceller and simulator, respectively, are uncorrelated random vectors, and that they are uncorrelated with each other. In addition, we assume that the canceller is long enough to cover the memory span of the echo channel, that the simulator is long enough to cover the memory span of the far-end-signal channel and, finally, that the delay element of Figure 2-1 does not affect performance.<sup>6</sup> We first define the echo residual at the equalizer input, i.e., the error in the near-echo estimate, as

$$e_o(nT) = \varepsilon_N(nT) - \hat{s}_N(nT) \quad (2-10a)$$

("o" denoting the echo estimates out of the cancellers) and the error in the far-end-signal estimate as

$$e_f(nT) = f(nT) - \hat{f}(nT) \quad (2-10b)$$

We also define the coefficient error vectors for the canceller and simulator, respectively, as

$$\underline{e}_a(nT) = \underline{a}_i(nT) - \underline{a}(nT) \quad (2-11a)$$

$$\underline{e}_b(nT) = \underline{b}_i(nT) - \underline{b}(nT) \quad (2-11b)$$

where "i" denotes the ideal coefficient vector. In addition, we shall denote the power in the canceller and simulator input symbol trains,  $\underline{x}(nT)$  and  $\underline{y}(nT)$  (which have the same power), the far-end signal,  $f(nT)$ , and white background noise,  $w(nT)$ , respectively, as  $P_x$ ,  $P_f$ , and  $P_w$ . We also let  $N_a$  and  $N_b$  denote the length of the canceller and simulator, respectively. From Equations (2-5b), (2-5c), (2-10), and (2-11), it is then straightforward to show that, if the successive data bits are uncorrelated, the mean-squared error at the equalizer input  $e_o(nT)$  can be related to the canceller-coefficient error as

$$E[e_o^2(nT)] = \frac{P_x E[\underline{e}_a^t(nT) \underline{e}_a(nT)]}{2} \quad (2-12a)$$

and the mean-squared error in the far-end signal is related to the simulator coefficient error as

$$E[e_f^2(nT)] = \frac{P_x E[\underline{e}_b^t(nT) \underline{e}_b(nT)]}{2} \quad (2-12b)$$

The approach to determining  $E[e_o^2(n)]$  requires a set of coupled recursions on  $E[e_o^2(n)]$  and  $E[e_f^2(n)]$ . We begin the derivation of echo residual power by writing recursively [from Equations (2-8) and (2-11)] the coefficient error vectors  $\underline{e}_a(nT)$  and  $\underline{e}_b(nT)$ :

$$\underline{e}_a[(n+1)T] = \underline{e}_a(nT) - \mu \underline{x}^*(nT) e(nT) \exp[-j\omega_c nT] \quad (2-13a)$$

$$\underline{e}_b[(n+1)T] = \underline{e}_b(nT) - \mu \underline{y}^*(nT) e(nT) \exp[-j\omega_c nT] \quad (2-13b)$$

where the residual error  $e(nT)$  was defined in Equation (2-5a), and where, for simplicity, we have set  $\mu = \mu_c = \mu_s$ . We next replace  $e(nT)$  in Equation (2-13) by a function of  $\underline{e}_a(nT)$  and  $\underline{e}_b(nT)$ .

Specifically, we can show that the error  $e(nT)$  can be written in terms of the difference between the actual echo and its estimate, and the actual far-end signal and its estimate; i.e., from Equations (2-4), (2-5) and (2-11), we have

$$\begin{aligned}
e(nT) &= r(nT) - [\hat{s}_N(nT) + \hat{f}(nT)] \\
&= [s_N(nT) - \hat{s}_N(nT)] + [f(nT) - \hat{f}(nT)] + w(nT) \\
&= \text{Re}\{\underline{e}_a^t(nT) \underline{x}(nT) \exp[j\omega_c nT]\} \\
&\quad + \text{Re}\{\underline{e}_b^t(nT) \underline{y}(nT) \exp[j\omega_c nT]\} + w(nT) \\
&= \text{Re}[\underline{e}_a^t(nT) \underline{x}(nT) + \underline{e}_b^t(nT) \underline{y}(nT)] \exp[j\omega_c nT] + w(nT) \quad (2-14)
\end{aligned}$$

Substituting Equation (2-14) into (2-13), and with some tedious algebraic manipulation, we obtain the coupled recursions

$$\begin{aligned}
E\{\underline{e}_a^t[(n+1)T] \underline{e}_a^*[(n+1)T]\} &= \left[1 - \mu P_x + \frac{\mu^2 N_a P_x^2}{2}\right] E[\underline{e}_a^t(nT) \underline{e}_a^*(nT)] \\
&\quad + \frac{\mu^2 N_a P_x^2}{2} E[\underline{e}_b^t(nT) \underline{e}_b^*(nT)] + \mu^2 N_a P_x P_w \quad (2-15a)
\end{aligned}$$

and

$$\begin{aligned}
E\{\underline{e}_b^t[(n+1)T] \underline{e}_b^*[(n+1)T]\} &= \left[1 - \mu P_x + \frac{\mu^2 N_b P_x^2}{2}\right] E[\underline{e}_b^t(nT) \underline{e}_b^*(nT)] \\
&\quad + \frac{\mu^2 N_b P_x^2}{2} E[\underline{e}_a^t(nT) \underline{e}_a^*(nT)] + \mu^2 N_b P_x P_w \quad (2-15b)
\end{aligned}$$

Finally, combining Equations (2-12) and (2-15), we have the desired coupled recursions on  $E[e_o^2(nT)]$  and  $E[e_f^2(nT)]$

$$\begin{aligned}
E\{e_o^2[(n+1)T]\} &= \left[1 - \mu P_x + \frac{\mu^2 N_a P_x^2}{2}\right] E[e_o^2(nT)] \\
&\quad + \frac{\mu^2 N_a P_x^2}{2} E[e_f^2(nT)] + \frac{\mu^2 N_a P_x^2 P_w}{2} \quad (2-16a)
\end{aligned}$$

$$\begin{aligned}
E\{e_f^2[(n+1)T]\} &= \left[1 - \mu P_x + \frac{\mu^2 N_b P_x^2}{2}\right] E[e_f^2(nT)] \\
&\quad + \frac{\mu^2 N_b P_x^2}{2} E[e_o^2(nT)] + \frac{\mu^2 N_b P_x^2 P_w}{2} \quad (2-16b)
\end{aligned}$$

Solving the (two-dimensional) recursion (2-16) at steady state, and selecting the echo residual at the equalizer input (in a style similar to Reference 6), we obtain the signal-to-echo ratio (denoted by  $S/E_0$ ) as

$$S/E_0 \approx \frac{P_f}{P_w} \frac{[2 - \mu(N_a + N_b) P_x]}{\mu N_a P_x} \quad (2-17)$$

where the convergence gain  $\mu = \mu_c = \mu_s$ . The steady state error, Equation (2-17), reduces to that found by Falconer<sup>6</sup> for the case of a bipolar input (with unity power) and real filter coefficients.

A VAX 780 computer simulation with floating-point arithmetic was used to evaluate the performance of the echo-cancelling modem. The simulated data rate was 4800 b/s. The modem signal uses four-phase, differential phase shift keying (DPSK) at 2400 bauds/s, an 1800-Hz carrier, and a 31-point pulse shape.<sup>11</sup> The signal is sampled at a 7200-Hz rate and the length of each of the adaptive filters is 88 samples. A telephone channel with average dispersion (50 samples or about 7 ms) was used in the simulation for both the far-end channel and echo path. The adaptive filters are sufficiently long to represent the composite signal formed by convolving the transmit pulse with this channel. The convergence gains for the canceller and the channel simulator were set at  $\mu_c = \mu_s = .05$ , and the convergence gain for the equalizer was set at  $\mu_e = .15$ . The initial adaptation takes place during a 2000 baud preamble in which the far-end symbols are known *a priori*. Adaptation of the canceller and channel-simulator coefficients begins at the onset of the preamble, while the adaptation of the equalizer coefficients is initiated 1500 bauds into the preamble; this timing scenario allows the echo to be significantly reduced before beginning equalizer adaptation. The resulting far-end-signal-to-echo as a function of time,  $S/E_0(t)$ , was measured by averaging the squared echo residual at the equalizer input of Figure 2-1; this averaging was taken over a 35 ms or 84 baud interval.

Figure 2-2 gives a comparison of the dynamic behavior of the system with and without the adaptive reference (i.e., "zero reference" <sup>6</sup>) for an original echo-to-signal ratio of 40 dB, and a signal-to-noise ratio (S/N) of 20 dB in the received signal. The adaptive zero reference canceller (ZREC) is formed by disabling the channel simulator in Figure 2-1 so that the far-end signal estimate is not subtracted from the echo residual. As expected, with all parameters held fixed the AREC system performs significantly better than its ZREC counterpart. The observed steady-state values were obtained by averaging over the steady-state regions of the curves. Equation (2-17) predicts a steady-state value of 25.38 dB, a good match to the measured  $S/E_0 \approx 25.22$  dB.

Table I shows the measured and predicted steady-state performance of the echo-cancelling modem algorithms with and without adaptive reference for an S/N of 30 and 20 dB, and an echo-to-far-end-signal ratio running from -20 dB to 60 dB in increments of 20 dB. The predicted zero reference  $S/E_0$  was obtained from Weinstein,<sup>2</sup> and the measured and predicted values were rounded to the nearest integer dB. As expected, the ZREC algorithm does considerably worse than its AREC counterpart in reducing the echo for all noise and echo levels. Table I also confirms the analytical predictions that performance is not a function of the original echo-to-far-end-signal ratio, but is limited by the noise level. For a fixed value of convergence rate,  $\mu$ , the echo is suppressed to the same level relative to the noise.



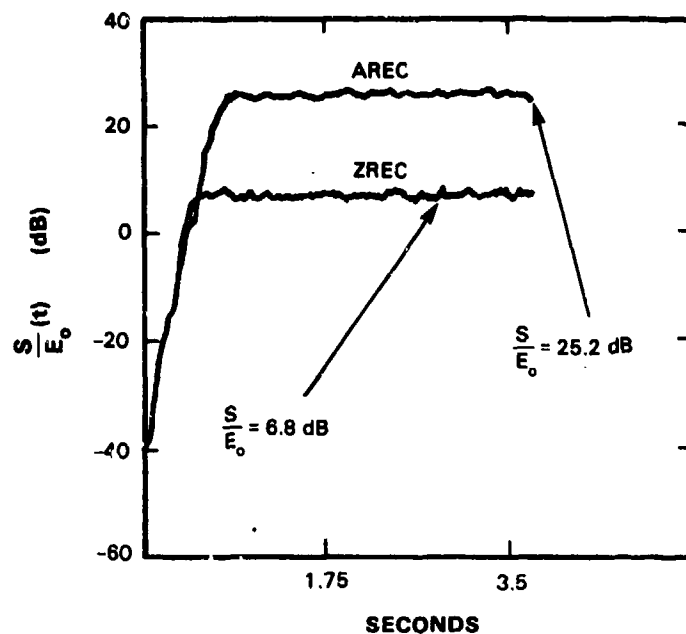


Figure 2-2. Performance of echo-cancelling modem algorithm with and without adaptive reference at 4800 b/s.

<b>TABLE I</b> <b>Measured and Predicted <math>S/E_0</math> (dB) for Echo-Cancelling Modem Algorithm With and Without Adaptive Reference at 4800 b/s</b>						
$E_i/S$ <b>S/N</b>	<b>Simulated</b>					<b>Pred</b>
	-20	0	20	40	60	*
30	35	35	35	35	35	35
	7	7	7	7	7	7
20	25	25	25	25	25	25
	7	7	7	7	7	7

AREC
ZREC

### 2.3 The Effect of Frequency Offset

We have seen that the AREC system can accommodate the near echo when the far-end signal and echo paths are given by a linear time-invariant channel. A problem arises, however, when the echo (i.e., the far echo) and far-signal paths are disturbed by carrier phase distortions. In particular, carrier frequency offset can be the most damaging to far-echo cancellation.<sup>1</sup> We will focus on this distortion within the remainder of the report.

Frequency offset arises from baseband/passband frequency translations in the long-haul carrier transmission. One can interpret this effect as a continuous rotation of the complex coefficients of the channel response. This can be seen by rewriting Equation (2-2) with only its frequency offset component:

$$\begin{aligned} s(nT) &= \text{Re} \left\{ \sum_k I_k g[(n - kL)T] \exp[j\omega_0 nT] \exp[j\omega_c nT] \right\} \\ &= \text{Re} \left\{ \sum_k I_k g'(nT, kLT) \exp[j\omega_c nT] \right\} \end{aligned} \quad (2-18a)$$

where  $g'(nT, kLT)$  is a time-varying filter given by

$$g'(nT, \tau T) = g[(n - \tau)T] \exp[j\omega_0(n - \tau)T] \exp[j\omega_c \tau T] \quad (2-18b)$$

The transformed impulse response  $g'(nT, \tau T)$  can be interpreted as a linear time-invariant response  $g(nT) \exp[j\omega_0 nT]$  multiplied by the time-varying component  $\exp[j\omega_c \tau T]$  for an impulsive input at time  $\tau T$ . Thus, the complex coefficients of the transformed response are continuously being rotated at the rate  $\omega_c$ . The adaptive (LMS) algorithm of Equation (2-8) must then be fast enough to track this rotation. However, Equation (2-7) shows that increasing the convergence gain to speed the adaptation decreases the echo suppression.

Figure 2-3 illustrates the behavior of the AREC modem algorithm for a 2-Hz frequency offset that was introduced into the echo carrier at 3000 bauds from the time origin. All parameters are given, as in the simulations described above, in Section 2.2. The original echo-to-signal ratio for this example is set at -10 dB (typical for far echo) and S/N equals 20 dB. The canceller tap weights rotate in an attempt to track the linearly advancing phase. Nevertheless, the canceller's complex taps track the channel impulse response with a fixed phase lag which prevents the cancellation from reaching the earlier high suppression level. As shown in Figure 2-3, an increase in the convergence gain to  $\mu_c = .075$  tends to increase the echo suppression during the frequency offset by improving the tracking capability of the canceller; however, the echo suppression is worse before the introduction of the frequency offset. Similar performance degradation occurs with the channel simulator when frequency offset is introduced in the far-end signal.

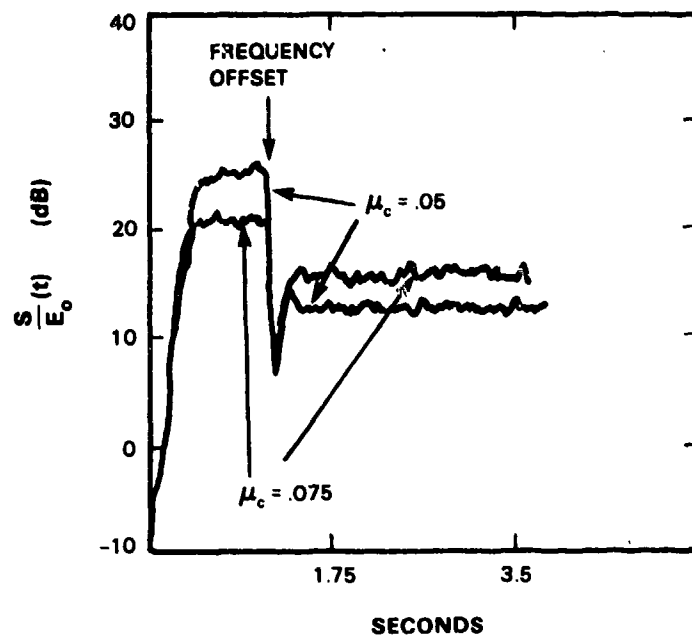


Figure 2-3. Effect of convergence gain on AREC response with far-echo frequency offset.

77437-2

### 3. ADAPTIVE-REFERENCE ECHO CANCELLATION WITH FREQUENCY OFFSET ESTIMATION

In this section, we present a design for a full-duplex adaptive-reference echo-cancelling modem which can compensate for near and far echoes when frequency offset is present in both the far echo and the far-end signal. We begin with an adaptive-reference near- and far-echo canceller with a known frequency offset. We then extend this method to develop the full echo-cancelling modem design by addressing first the frequency offset in the far-end signal and, finally, offset in the far echo.

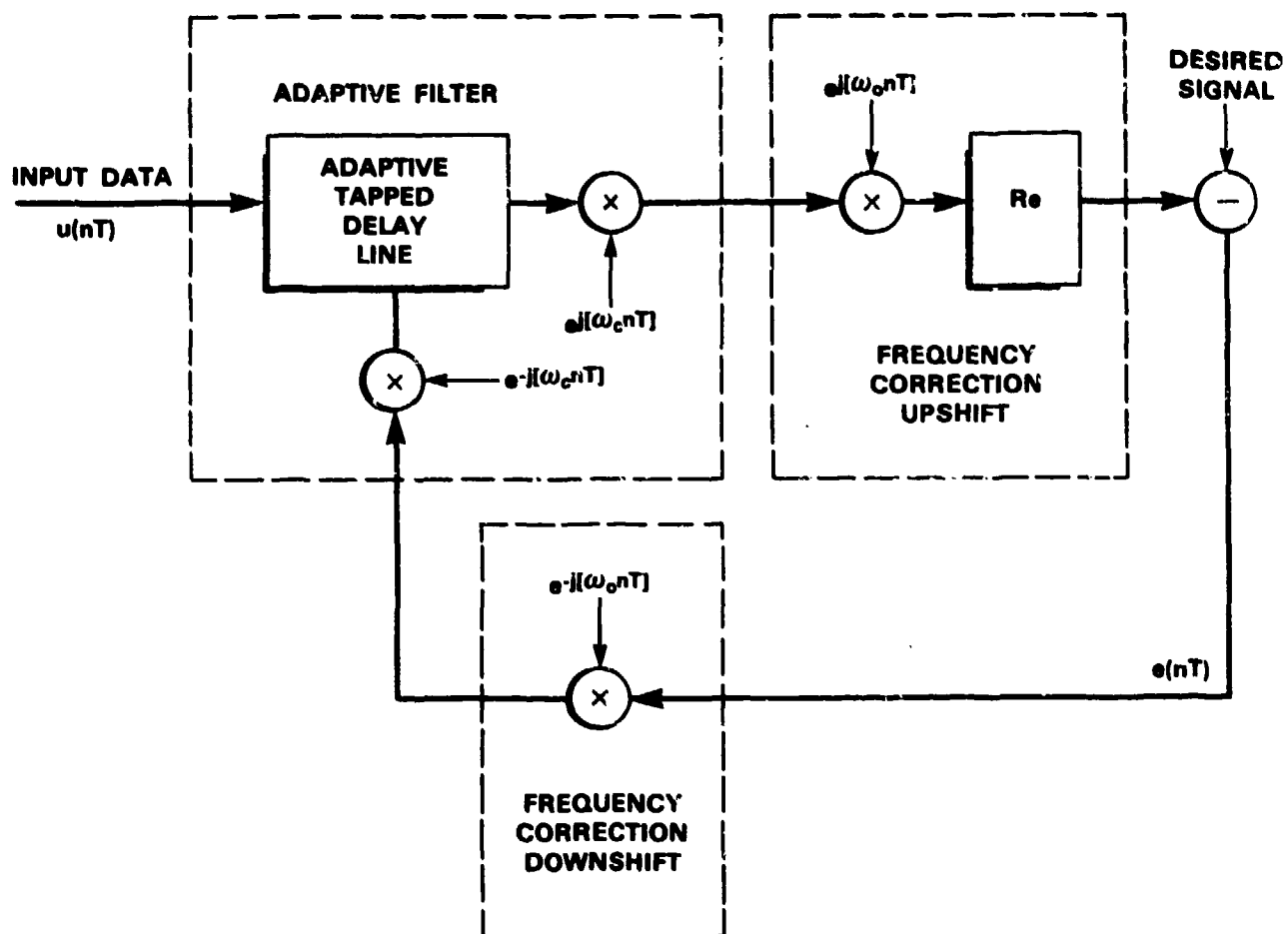
#### 3.1 Cancellation with a Known Frequency Offset

If the far-end signal and far echo are received with a known frequency offset, then the echo-cancelling modem (i.e., the channel simulator and echo canceller) must reproduce these signals with the same offset in order to perform adequate cancellation. In this case the adaptive filtering procedure is no different than before, since we can interpret the sum of the known carrier and known offset as a new carrier. Figure 3-1 illustrates an adaptive procedure for approximating a passband signal with a known offset,  $\omega_o$ . This structure minimizes the mean-squared-error  $e(nT)$  between the modulated filter output and the desired signal. The signal is generated, as before, by a complex tapped delay line, followed by a translation to passband. However, in this case an additional shift up by the known frequency offset is included in the translation, thus changing the effective carrier. The corresponding downshift in the error signal is also provided. For simplicity in representing the more complex systems to follow, we have segmented the adaptive structure into three primary modules: an adaptive filter which includes signal modulation and error demodulation by the carrier, carrier frequency correction "downshift" for the error signal, and carrier frequency correction "upshift" which includes the real-component operator. The LMS update for the filter coefficient vector  $\underline{h}(nT)$  is given by

$$\underline{h}[(n+1)T] = \underline{h}(nT) + \mu \underline{u}^*(nT) e(nT) \exp[-j(\omega_c + \omega_o) nT] \quad (3-1)$$

where  $\underline{u}(nT)$  is the input data vector. The phase rotation of the error residual uses the original carrier phase modified by the linear phase due to the known frequency offset. The derivation of Equation (3-1) is similar in style to that used in Equations (2-6) through (2-8).

Figure 3-2 shows the design for an adaptive-reference near- and far-echo-cancelling modem based on the building blocks of Figure 3-1. The design accommodates known frequency offsets in both the far-end signal and far echo. These offsets are denoted by  $\omega_{os}$  and  $\omega_{oe}$ , respectively. The corresponding linear phase corrections are denoted by  $\theta(nT) = \omega_{os}nT$  and  $\phi(nT) = \omega_{oe}nT$ . Both the near-echo and far-echo adaptive cancellers and channel simulator are driven by the residual  $e(nT)$ , obtained by subtracting the far-end-signal estimate and the two echo estimates from the received signal. Thus, the far-end signal is eliminated as a source of interference to either the near-echo or far-echo canceller adaptation. In addition, the far echo is not a source of interference to the adaptation of the near-echo canceller and vice versa. The error residual  $e(nT)$ , with the independent corrections one would expect from Figure 3-1, drives the three adaptations.



77437-5

Figure 3-1. Adaptive structure for replicating a passband modem signal with a known frequency offset.

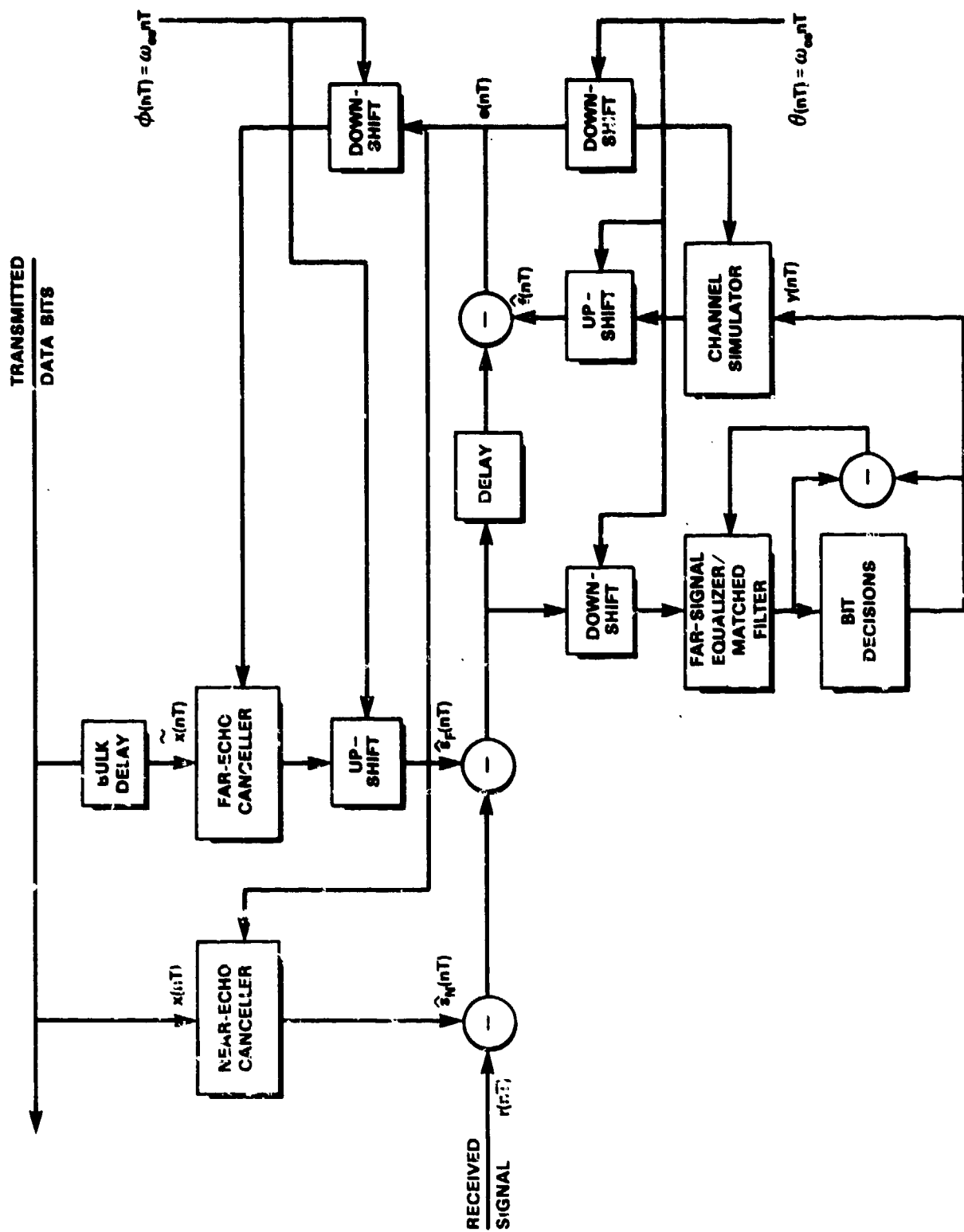


Figure 3-2. Canceller with far-echo cancellation and known frequency offsets in far echo and far-end signal.

Likewise, the outputs of the channel simulator and cancellers are translated to passband by separately corrected carriers. In addition, the demodulator of the channel equalizer is corrected by the far-end-signal frequency offset. A bulk delay is introduced before the far-echo canceller to account for the roundtrip delay time of the transmitted signal, and thus reduces the required number of taps in the far-echo canceller.

All three coefficient sets are updated as in Equation (3-1). A derivation of these joint adaptive update procedures parallels that of Section 2.2 and begins by minimizing the average-squared residual  $e(nT)$  formed by subtracting the far echo, near echo, and far-end signal estimates from the received signal:

$$e(nT) = r(nT) - [\hat{s}_N(nT) + \hat{s}_F(nT) + \hat{f}(nT)] \quad (3-2)$$

Where the near-echo estimate  $\hat{s}_N(nT)$  is defined in Equation (2-5b). The far echo estimate is given by

$$\hat{s}_F(nT) = \text{Re}\{\tilde{\mathbf{x}}^t(nT) \tilde{\mathbf{a}}(nT) \exp[j[\omega_c nT + \phi(n)]]\} \quad (3-3)$$

where the vector  $\tilde{\mathbf{x}}(nT)$  denotes the (bulk) delayed near-end symbol train (see Figure 3-2), where  $\tilde{\mathbf{a}}(nT)$  denotes the far-echo-canceller coefficients, and where the phase  $\phi(nT) = \omega_{oc}nT$  accommodates frequency offset in the far echo. The far-end signal estimate  $\hat{f}(nT)$  is given by

$$\hat{f}(nT) = \text{Re}\{\mathbf{y}^t(nT) \mathbf{b}(nT) \exp[j[\omega_c nT + \theta(nT)]]\} \quad (3-4)$$

where we have included the phase correction term  $\theta(nT) = \omega_{os}nT$  in the far-end-signal modulator to accommodate the frequency offset in the channel carrier. We wish to solve the problem

$$\text{minimize } E[|e(nT)|^2] \quad (3-5)$$

over the coefficient vectors  $\mathbf{a}(nT)$ ,  $\tilde{\mathbf{a}}(nT)$ , and  $\mathbf{b}(nT)$  under the condition that  $\phi(nT)$  and  $\theta(nT)$  are known. The LMS algorithm can be used to solve Equation (3-5) by approximating the gradient of  $E[|e(nT)|^2]$  with respect to all three parameter sets by using the "instantaneous gradient" measure to obtain

$$\mathbf{a}[(n+1)T] = \mathbf{a}(nT) + \mu_c \mathbf{x}^*(nT) e(nT) \exp[-j\omega_c nT] \quad (3-6a)$$

$$\tilde{\mathbf{a}}[(n+1)T] = \tilde{\mathbf{a}}(nT) + \mu_c \tilde{\mathbf{x}}^*(nT) e(nT) \exp\{-j[\omega_c nT + \phi(nT)]\} \quad (3-6b)$$

and

$$\mathbf{b}[(n+1)T] = \mathbf{b}(nT) + \mu_s \mathbf{y}^*(nT) e(nT) \exp\{-j[\omega_c nT + \theta(nT)]\} \quad (3-6c)$$

where, as proposed in Figure 3-2, the residual  $e(nT)$  is mixed by three distinct factors before driving the various coefficient adaptations.

### 3.2 Adaptive-Reference Near-Echo Cancellation with Unknown Frequency Offset in the Far-End Signal

In practice, the far-end-signal frequency offset is unknown and must be estimated. Figure 3-3 illustrates the adaptive-reference near-echo-cancelling modem design which estimates far-end-signal frequency offset. The offset estimator is part of the receiver structure which performs joint

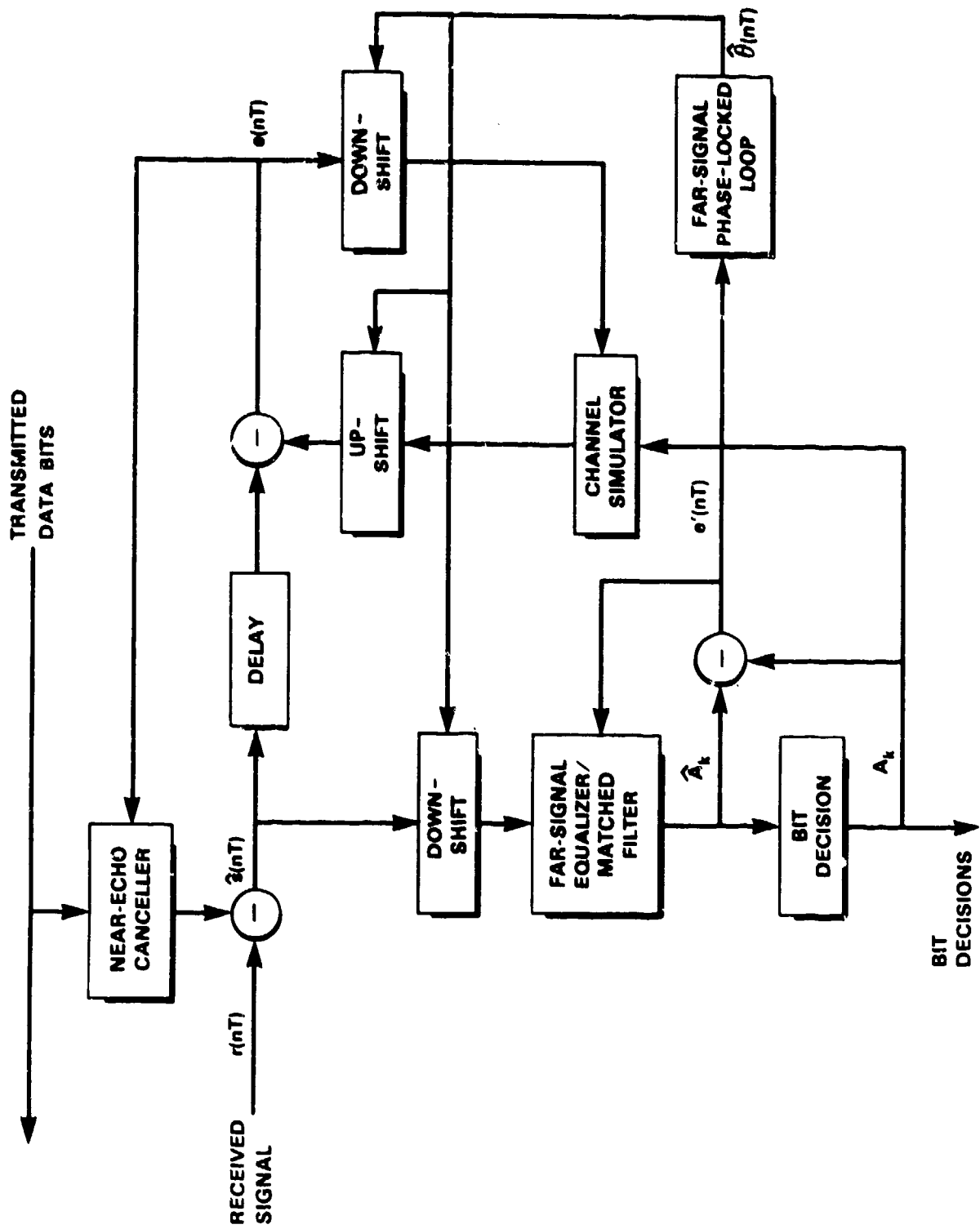


Figure 3-3. Canceller with correction for frequency offset in far-end signal.



adaptive equalization/matched filtering. The technique is similar to that used in other receivers which perform joint equalization and carrier recovery.<sup>12,13</sup> The decision error residual  $e'(nT)$  driving the equalizer is also used by the phase-tracking loop to provide an estimate  $\hat{\theta}(nT)$  of the phase due to the offset. The output of the phase-locked loop is used to correct the input to the equalizer, the output of the channel simulator, and the error residual controlling the channel simulator.

To obtain the far-end-channel phase correction  $\theta(nT) = \omega_{os}nT$ , we minimize with respect to the unknown equalizer coefficients  $\underline{c}(nT)$  and frequency offset  $\omega_{os}$ , the decision error,  $e'(nT)$ , evaluated at the baud intervals between the far-end symbols  $\hat{A}_k$ , determined by the bit decisions and the far-end symbol estimates  $\hat{A}_k$ :

$$e'[(n = kL)] = \hat{A}_k - A_k \quad (3-7a)$$

with

$$\hat{A}_k = \underline{z}^t(nT) \underline{c}(nT) \big|_{nT = kLT} \quad (3-7b)$$

where  $\underline{z}(nT)$  is the phase corrected input to the equalizer:

$$\underline{z}(nT) = [r(nT) - \hat{s}(nT)] \exp \{-j[\omega_c nT + \theta(nT)]\} \quad (3-7c)$$

To further generalize the optimization, we allow for an unknown constant (as well as linear) component to the phase compensation  $\theta(nT)$ , i.e.,  $\theta(nT) = \omega_{os}nT + \theta_0$ . Although the adaptive filters, being complex, can account for a constant phase offset, this generalization takes some burden off the adaptive filters and also leads to a conventional phase-tracking structure whose properties have been extensively studied.<sup>12,13,14,15</sup> The minimization problem we wish to solve is given by

$$\text{minimize } E[|e'(nT)|^2] \quad (3-8)$$

over  $\underline{c}(nT)$ ,  $\omega_{os}(nT)$ , and  $\theta_0(nT)$  which appear via Equation (3-7). This problem can be simplified by assuming that the phase correction  $\theta(nT)$  is approximately constant over the time span of the equalizer/matched filter. This "quasi-stationary" assumption, assured if the frequency offset  $\omega_{os}N_b T \ll 1$ , leads to an LMS iterative solution (gradient search) to (3-8), with updates occurring at the baud rate. The solution, derived in a style similar to that in References 12, 13, and 14, is given by

$$\underline{c}[(k+1)LT] = \underline{c}(kLT) + \mu_e e'(kLT) \underline{z}(kLT) \quad (3-9a)$$

$$\hat{\theta}[(k+1)LT] = \hat{\theta}(kLT) + \omega_{os}(kLT) + k_1 \Delta \xi(kLT) \quad (3-9b)$$

with

$$\omega_{os}[(k+1)LT] = \omega_{os}(kLT) + k_2 \Delta \xi(kLT) \quad (3-9c)$$

$$\Delta \xi(kLT) = \sin[\hat{\xi}(kLT) - \xi(kLT)] \quad (3-9d)$$

and where  $\xi(kLT)$  and  $\hat{\xi}(kLT)$  denote the phase of the complex far-end symbol  $A_k$  and its estimate  $\hat{A}_k$ , respectively. Equations (3-9b) to (3-9d) represent a second-order phase-locked loop whose stability properties are discussed in Reference 14.

### 3.3 Adaptive-Reference Far-Echo Cancellation with Frequency Offset in the Far Echo

The same type of phase correction as in Equation (3-9) could be employed to correct the frequency error in the far echo. The difficulty is that the far echo is typically smaller (-10 dB) than the far signal, but of the same form. To overcome this difficulty we must first enhance the visibility of the far echo. An estimate of the far echo is formed by subtracting from the received signal an estimate of the near echo and the far signal as depicted in Figure 3-4. As before, a delay is incorporated prior to determining the far-echo estimate to account for the processing time required by the channel equalizer and channel simulator. This procedure improves the far-echo-to-interference ratio enough that we can then use another adaptive equalizer/matched filter structure identical to that used for the far-end signal. The goal of this receiver is to demodulate the far echo. However, since we are dealing with an echo, the task is considerably easier because the bit decisions are already known. Thus the transmitted bits, suitably delayed, can be used in the determination of the error signal  $e''(nT)$  out of the receiver. The bulk delay provides delay approximately equal to the round-trip channel delay. This delay needs to be estimated as part of the initial training.

This error residual  $e''(nT)$  drives the far echo equalizer/matched filter adaptation, thus adapting for the dispersion over the echo path. The error formed at the baud rate is  $e''(nT = kLT) = \hat{I}_k - I_k$ ,  $I_k$  being the near-end symbol and  $\hat{I}_k$  being the near-end symbol estimate. Thus, the equalizer adaptation occurs at the baud rate. The error residual  $e''(nT)$  also drives the phase-tracking algorithm which results in the estimate  $\hat{\phi}(nT)$  containing a linearly changing phase due to frequency offset in the far echo. The phase estimate  $\hat{\phi}(nT)$  is used to correct the frequency of the far-echo canceller output, the frequency of the input to the far-echo equalizer/matched filter, and the phase of the error signal driving the far-echo canceller.

The detailed analysis for the phase-tracking and equalizer/matched filter coefficient update is exactly the same as in Section 3.2 [Equations (3-7) to (3-9)], except that the far-echo bit pattern is known exactly and need not depend on the receiver decisions. As with the far-signal frequency-offset estimation, by minimizing the mean-squared  $e''(nT)$ , we can derive a set of coupled update equations of the form (3-9). The error at the echo receiver output is used to drive the adaptive LMS update of the equalizer coefficients and the second-order phase-locked loop which drives the carrier compensation.

### 3.4 The Composite System

The entire modem design, merging Figures 3-3 and 3-4, is illustrated in Figure 3-5 where we have included the phase tracking required for estimating frequency offsets in both the far-end signal and the far echo. The composite system requires two adaptive cancellers, one adaptive channel simulator, two adaptive equalizers, and two phase-tracking loops. The updates for the canceller and simulator filter coefficients are given by Equation (3-6) and the phase tracking and equalization is given by Equation (3-9) (the far-echo receiver also being of this form). The error



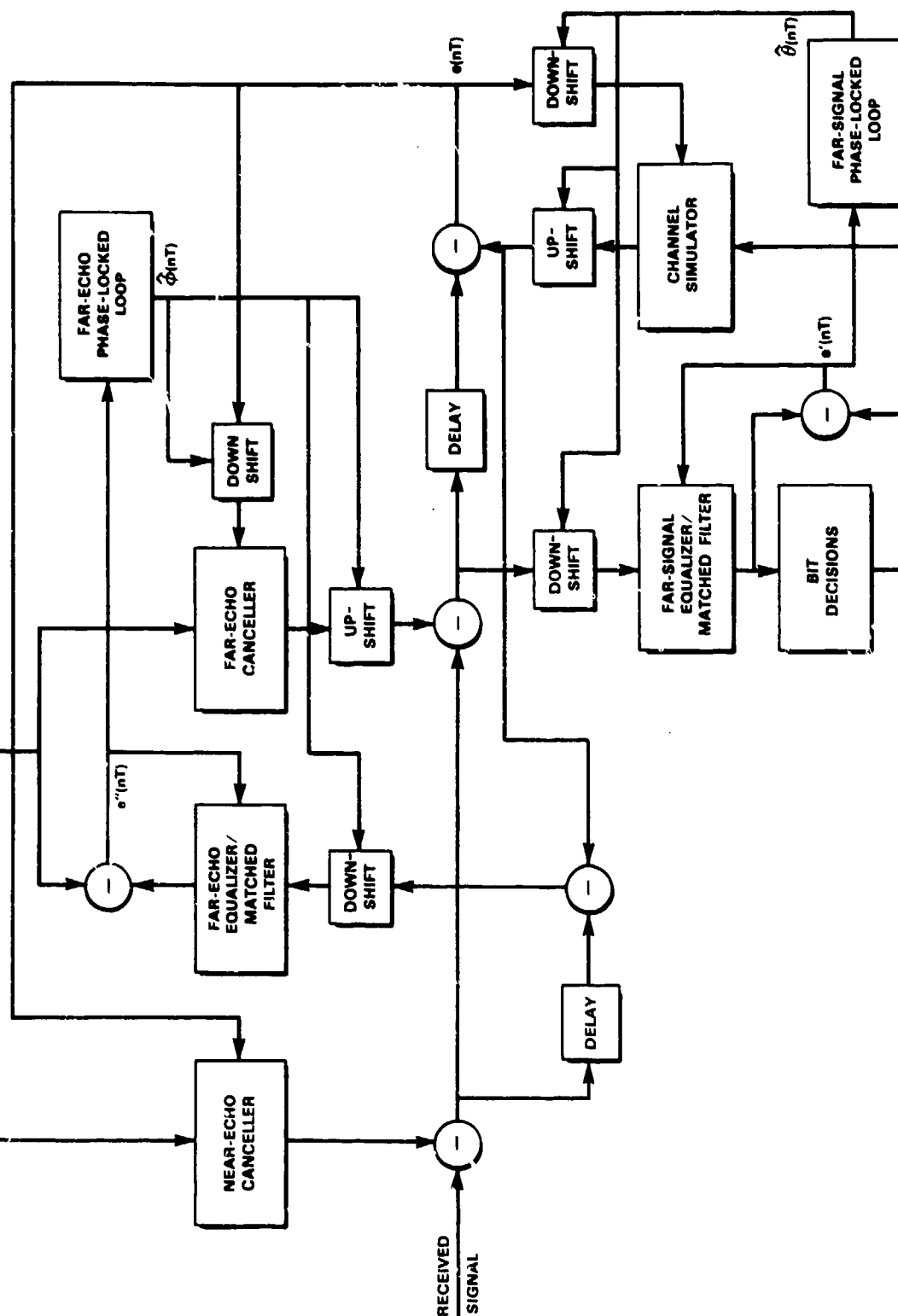


**Figure 3-5. Cancellor with correction for fare-echo and far-signal frequency offset.**

residual  $e(nT)$ , which drives the two cancellers and the simulator, is mixed with different carrier frequency corrections: one for the channel simulator with a phase correction,  $\hat{\theta}(nT)$ , derived from the phase-locked loop attached to the far-end-channel equalizer; one for the far-echo canceller with a phase correction,  $\hat{\phi}(nT)$ , derived from the phase-locked loop attached to the far-echo-path equalizer. The errors driving the far-end-channel equalizer and far-echo-path equalizer and their corresponding phase-tracking algorithms are formed from their respective "decision distances,"  $e'(nT)$  and  $e''(nT)$ .

The approximate steady-state performance (the dynamic performance is beyond the scope of this report) of the composite near- and far-echo canceller can be determined by using the result of Section 2.2, and by viewing the two cancellers as one long "linear combiner,"<sup>10</sup> which attempts to estimate the sum of the near and far echoes. We also assume that the frequency offset estimates have settled to their correct values. We then define a new canceller coefficient vector  $A(nT)$

$$A(nT) = [\underline{a}(nT) \ \tilde{\underline{a}}(nT)]^t \quad (3-10a)$$

and a new input data vector

$$X(nT) = [\underline{x}(nT) \ \tilde{\underline{x}}(nT)]^t. \quad (3-10b)$$

Since a bulk delay separates the inputs  $x(nT)$  and  $\tilde{x}(nT)$ , the composite input vector  $X(nT)$  satisfies the previous independence assumption (i.e., successive data vectors are uncorrelated). When the near- and far-echo-canceller lengths are equal, the length of the new canceller coefficient vector  $X(nT)$  is  $2N_a$ , where  $N_a$  was defined earlier as the length of the near-echo canceller. Since we have replaced the vectors  $\underline{a}(nT)$  and  $\underline{x}(nT)$  of length  $N_a$  by the vectors  $A(nT)$  and  $X(nT)$  of length  $2N_a$ , the result of Section 2.2 can be used to obtain the approximate steady-state signal-to-echo ratio at the input to the far-end channel equalizer:

$$S/E_o \approx \frac{P_f}{P_w} - \frac{[2 - \mu(2N_a + N_b) P_x]}{2\mu N_a P_x} \quad (3-11)$$

where  $\mu = \mu_c = \mu_s$  and which we shall see in the following section is an accurate prediction of steady-state performance.

The receiver's adaptive structures are started sequentially during a 2000 baud training preamble. The timing scenario for adaptation over this preamble was determined according to relative signal levels and is illustrated in Figure 3-6. Since the near echo is the largest contribution to the received signal, the near-echo canceller adaptation begins at the onset of operation. After 700 bauds, following reduction of the near echo, the far-end-channel equalizer and its associated phase-locked loop (PLL) are started. At 1000 bauds the channel-simulator adaptation is begun. This gives the phase-locked loop some time to estimate a frequency offset to be used by the channel simulator which starts its adaptation at 1000 bauds, and also allows time to make the far echo visible over the near echo and far-end signal. The far-echo equalizer and its associated phase-locked loop are started at 1400 bauds, followed finally by the far-echo canceller at 1700 bauds. The far echo is cancelled last, since it is the smallest of the received signal components.

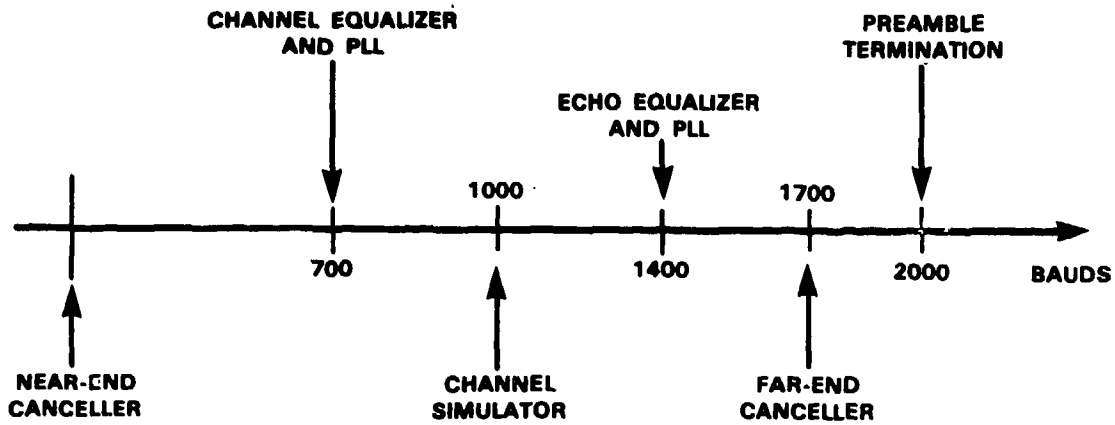


Figure 3-6. Preamble timing scenario for near/far-echo-cancelling modem algorithm.

There is a strong symmetry which characterizes the modem structure of Figure 3-5. The far-end-channel receiver, i.e., its equalizer and its associated phase-locked loop, and the far-end channel simulator form a "module" which is essentially duplicated by the far-echo receiver, i.e., its equalizer and its associated phase-locked loop and far-echo canceller. This modularity lends itself to an efficient hardware implementation.

#### 4. EVALUATION OF THE NEAR- AND FAR-ECHO-CANCELLING MODEM ALGORITHM AT 4800 b/s

The simulation of the complete modem algorithm was made with the same specifications used in the simulation of the near-echo-cancelling modem algorithm of Section 2.2. Filter lengths, convergence gains, modem signal design, baud and bit rates, are all the same as in the previous experiments, and are listed in Table II. The preamble timing scenario of Figure 3-6 was used for training. The parameters of the second-order phase-locked loops, which were chosen to make the phase tracker's response critically damped,<sup>14,15</sup> are also given in Table II.

<b>TABLE II</b> <b>Design Specifications for</b> <b>Near/Far-Echo-Cancelling Modem Algorithm</b>	
<b>Modem Signal Specifications:</b>	
Signal Constellation:	Four-Phase DPSK
Baud Rate:	2400 Bauds/s
Sampling Rate:	7200 Hz
Carrier Frequency:	1800 Hz
Transmit Pulse:	31-Point (Raised Cosine Spectrum <sup>11</sup> )
Bit Rate:	4800 b/s
Preamble:	2000 Bauds
<b>Receiver Specifications:</b>	
Adaptive Filter Lengths:	$N = 88$ taps
Near Echo/Far Echo Canceller Convergence Gains:	$\mu_c = .05$
Simulator Convergence Gain:	$\mu_s = .05$
Far-End Channel/Echo Path Equalizer Convergence Gains:	$\mu_e = .15$
Phase-Locked Loop Parameters: $k_1 = 1/64$ , $k_2 = 1/16384$	

We evaluate the new modem design in three stages. The system is first evaluated with no carrier frequency offset in the far-end channel and with and without near echo present. We then introduce carrier frequency offset in both the far echo and the far-end signal under a variety of

additive noise conditions. Finally, we test the system under a set of severe operating conditions by adding phase hits and impulse noise in both the far echo and far-end signal.

#### 4.1 Frequency Offset in the Far-Echo Channel

In order to compare the new algorithm with the adaptive-reference algorithm of Sections 2.2 and 2.3, we first test the system without the presence of the near echo and with no frequency offset in the far-end signal. The near-echo canceller output and the far-end channel phase correction  $\theta(n)$  were both disabled. As in the example of Figure 2-3, a 2-Hz frequency offset was injected into the far echo at 3000 bauds, the echo-to-far-end-signal ratio is -10 dB and the far-end-signal-to-noise ratio is 20 dB. Figure 4-1 shows that the introduction of a 2-Hz frequency offset at 3000 bauds caused a marked initial decrease in suppression and a transient increase in decision errors. Nevertheless, the phase-locked loop quickly tracked the frequency offset and recovered the original suppression within about .5 s, for an improvement of almost 13 dB over the scheme of Figure 2-3.

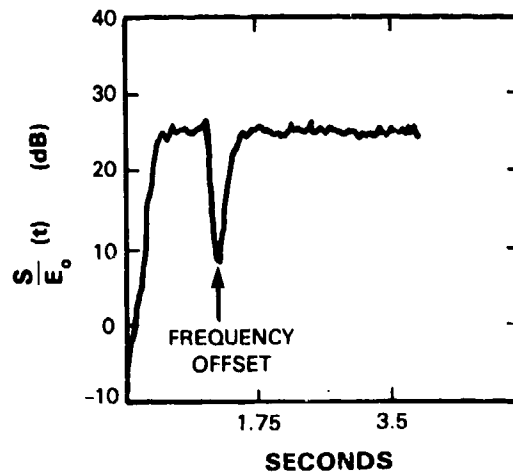
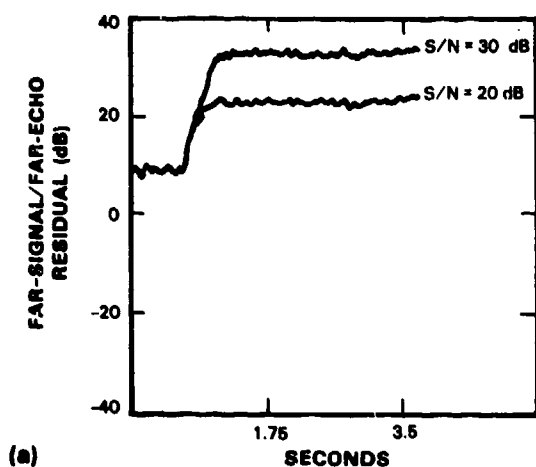
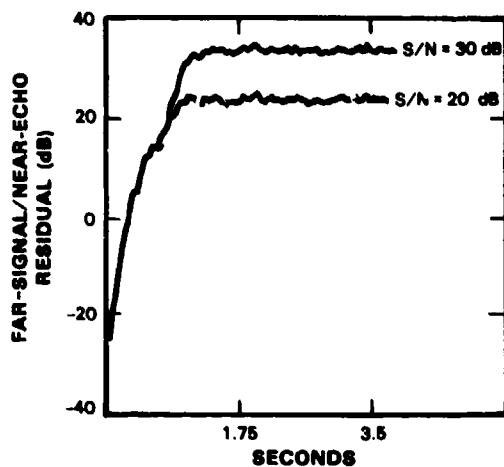


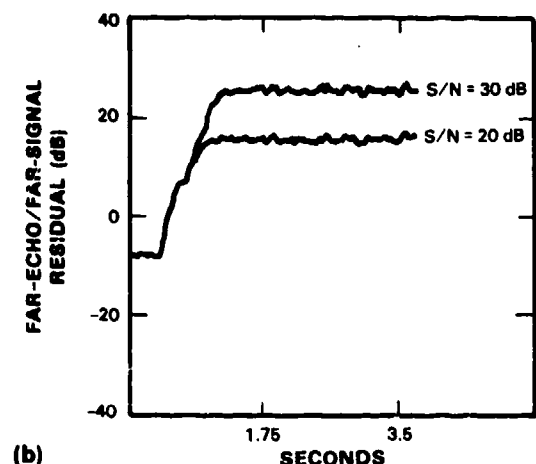
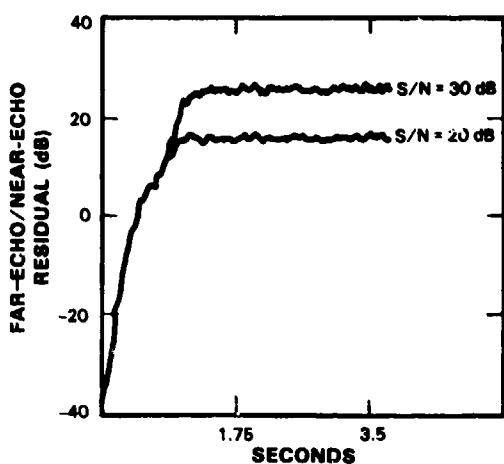
Figure 4-1. Performance of far-echo-cancelling modem algorithm (no near echo).

An evaluation of the complete far-echo-cancelling modem algorithm is depicted in Figure 4-2 with a near-echo-to-signal ratio of 30 dB, a far-echo-to-signal ratio of -10 dB, and  $S/N = 30$  dB and 20 dB. A 2-Hz frequency offset was introduced over the entire duration of the far echo. The far echo was formed by running the transmit signal through two average telephone channels, thus simulating the effects of the forward and backward channel paths. This far-echo path will be used throughout the remaining experiments. Although frequency offset was not introduced into the far-end channel signal, the phase-locked loop associated with the far-end channel equalizer was allowed to operate; the initial frequency offset was set to zero. All five adaptive filters successfully converged: two adaptive cancellers, the channel simulator, and the two adaptive equalizers, along with joint convergence of the phase-locked loop for estimation of the far-echo frequency offset. Figure 4-2 shows the dynamic performance of the canceller for this case. The most

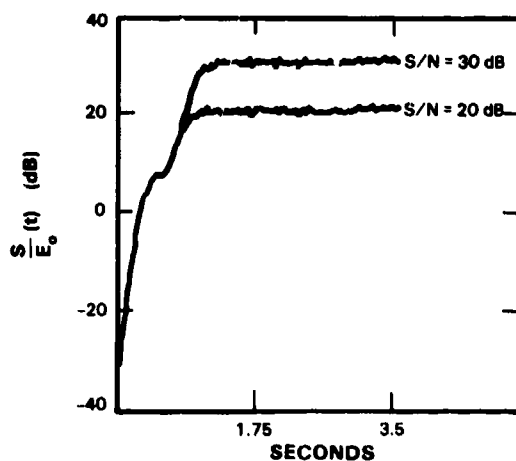




(a)



(b)



(c)

Figure 4-2. Error residuals of modem algorithm with frequency offset in far echo. (a) Residuals with respect to far signal at far-signal receiver, (b) Residuals with respect to far echo at far-echo receiver, (c) Signal-to-echo residual at equalizer input.

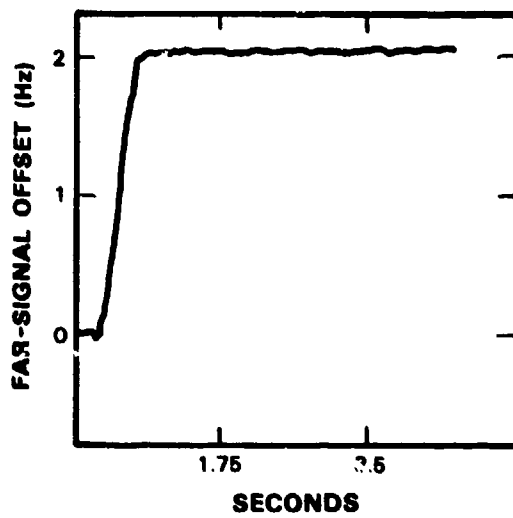
important consideration is, of course, the ability of the system to demodulate the incoming data. Figure 4-2(a) shows the signal-to-echo ratios at the input to the far-channel equalizer/matched filter. The suppression of the near echo starts immediately and continues until it is a few dB below the noise. The suppression of the far echo is delayed until the near echo has been suppressed, but is then quickly suppressed to about the same level. Figure 4-2(b) shows the suppression achieved at the input to the far-echo receiver. Here the interfering signals are the near echo and the far-end signal. Again, the amount of suppression achieved depends on the noise level. Figure 4-2(c) shows the combined near-and far-echo residual relative to the far-end signal at the far-channel equalizer input, i.e.,  $S/E_o$ , the signal-to-residual ratio which governs the ultimate error rate of the modem design. The steady-state results of Figure 4-2(c) approximately match those predicted from expression (3-11); for  $S/N = 30$  dB, we obtain a measured  $S/E_o \approx 30.6$  dB, close to the predicted 31.1 dB, and for  $S/N = 20$  dB, we obtain a measured  $S/E_o \approx 20.7$  dB, also close to the predicted 21.1 dB.

## 4.2 Frequency Offset in the Far Echo and Far-End Signal

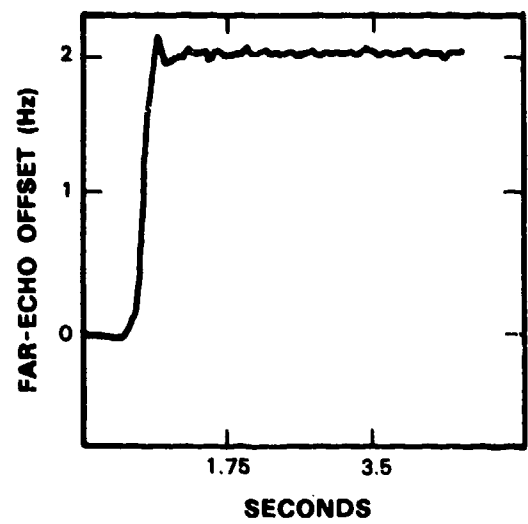
In the next set of experiments we introduce a 2-Hz frequency offset in the far-end signal as well as in the far echo. Figure 4-3(a) and 4-3(b) give the estimated frequency offsets in both signals, while Figure 4-3(c) shows the performance of the modem algorithm in terms of  $S/E_o$  for  $S/N = 30$  dB and 20 dB. In these experiments, the near-echo-to-signal ratio was 20 dB and the far-echo-to-signal ratio was -10 dB. All five adaptive filters successfully converged: two adaptive cancellers, the channel simulator, and the two adaptive equalizers, along with joint convergence of the two phase-locked loops for estimating frequency and phase offset. The results at convergence again approximately match those predicted from Equation (3-11); for  $S/N = 30$  dB, we obtain a measured  $S/E_o \approx 30.8$  dB close to the predicted 31.1 dB, and for  $S/N = 20$  dB, we obtain a measured  $S/E_o \approx 20.9$  dB, close to the predicted 21.1 dB. A  $S/N = 10$  dB appears to be the breaking point of the system. Here, we found that at the preamble termination,  $S/E_o$  is about 10 dB and still rising; its steady-state predicted value is about 12.4 dB. The signal-to-(noise + echo) ratio at the far-end-channel equalizer input was about 7 dB, which appears to be the borderline for making correct decisions with our particular far-end-channel receiver. A finer tuning of the parameter specifications may extend the range of successful use.

## 4.3 Other Channel Distortions

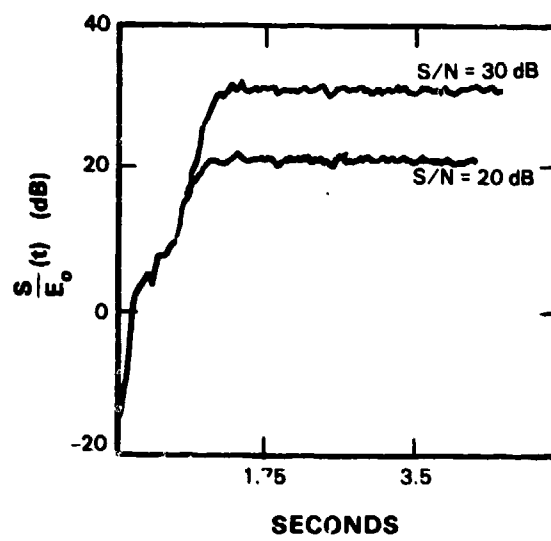
In the final test of this system we introduce carrier phase discontinuities into the channel. Such distortions can occur in carrier frequency translation. In particular, we introduce unidirectional phase hits (i.e., phase jumps that do not return to their original value), as well as a 2 Hz frequency offset to degrade both the far-end signal and the far echo. The echo levels are given as in the previous experiment with  $S/N = 20$  dB. The phase hits in the far echo are  $30^\circ$ ,  $80^\circ$ , and  $180^\circ$ , beginning at 3.75 s, and occurring in that order with about a 4-s spacing. The phase hits are depicted in Figure 4-4 by  $\theta_k^e$ . Since the far-echo-equalizer output is compared against known near-end symbols, a phase hit of  $180^\circ$  (or any odd multiple of  $180^\circ$ ) represents a worse case hit.



(a)

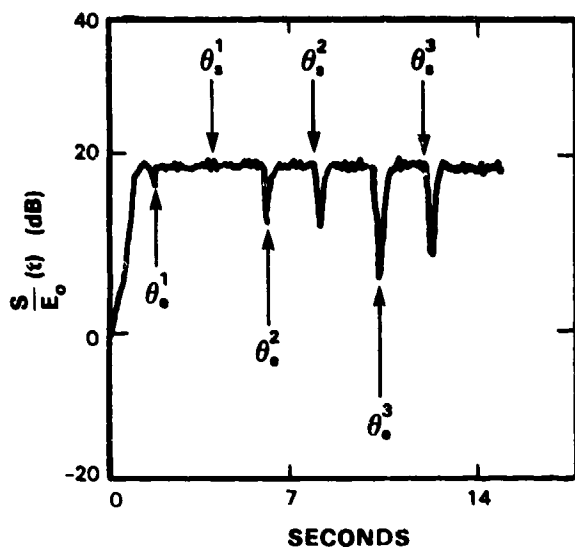


(b)

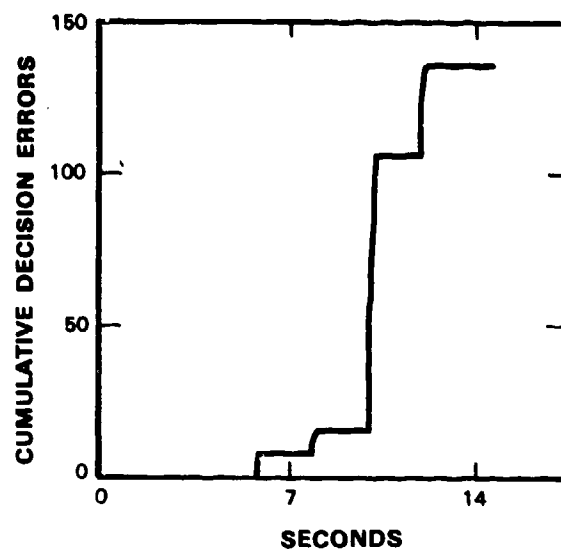


(c)

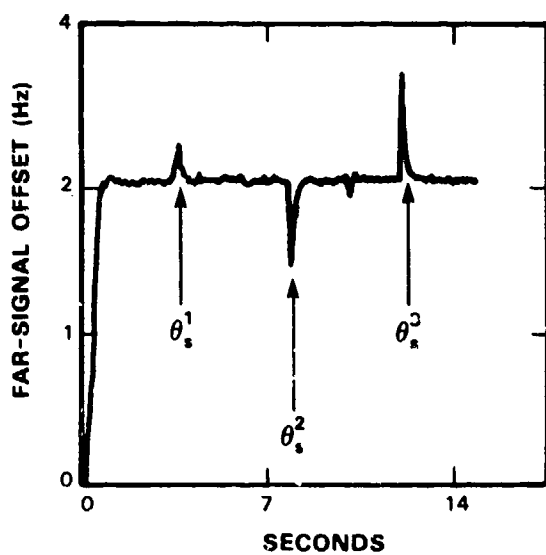
Figure 4-3. Response of modem algorithm with frequency offset in far signal and far-echo paths. (a) far-end-signal frequency-offset, (b) far-echo frequency offset, (c)  $S/E_0$ .



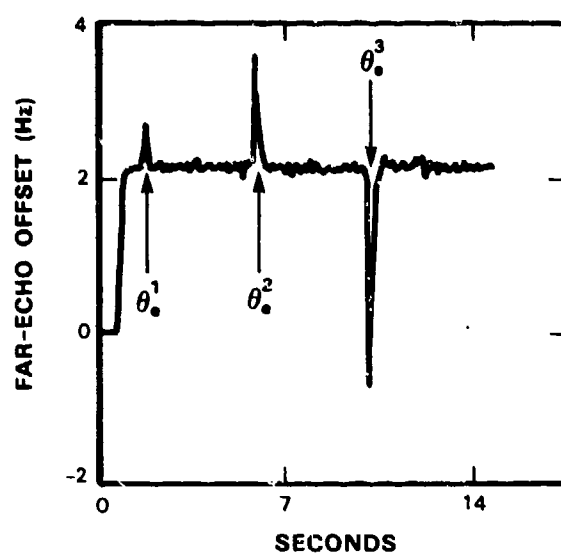
(a)



(b)



(c)

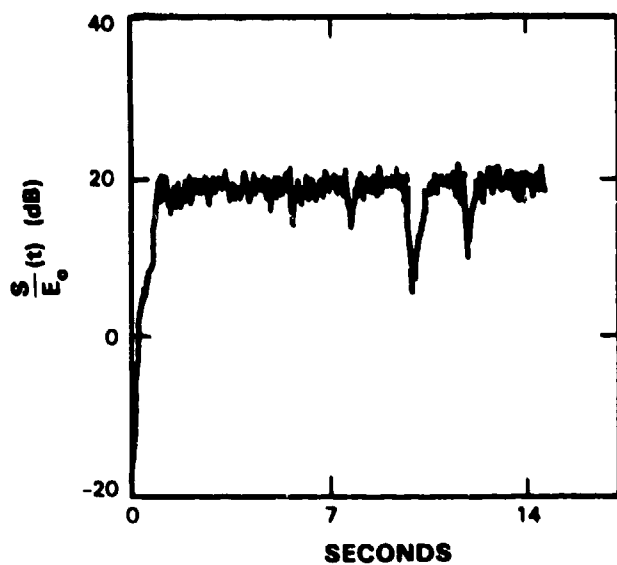


(d)

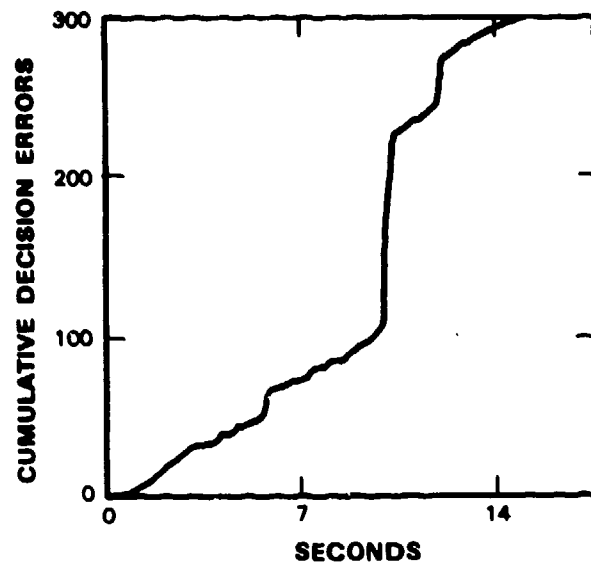
Figure 4-4. Performance of complete modem design with phase hits. (a)  $S/E_0$ , (b) accumulated receiver errors, (c) far-end-signal frequency-offset estimate, (d) far-echo frequency offset.

The phase hits in the far-end signal are  $15^\circ$ ,  $-40^\circ$ , and  $135^\circ$ , beginning at about 1.65 s and occurring in that order with about a 4-s spacing. The phase hits are depicted in Figure 4-4 by  $\theta_k^f$ . Since the far-end-signal receiver makes decisions on the far-end symbols on a constellation of decision points spaced by  $90^\circ$ , a phase hit of  $45^\circ$  (or any odd multiple of  $45^\circ$ ) represents a worse case hit. Figure 4-4 shows that the system recovers from these distortions and from the resulting decision errors.

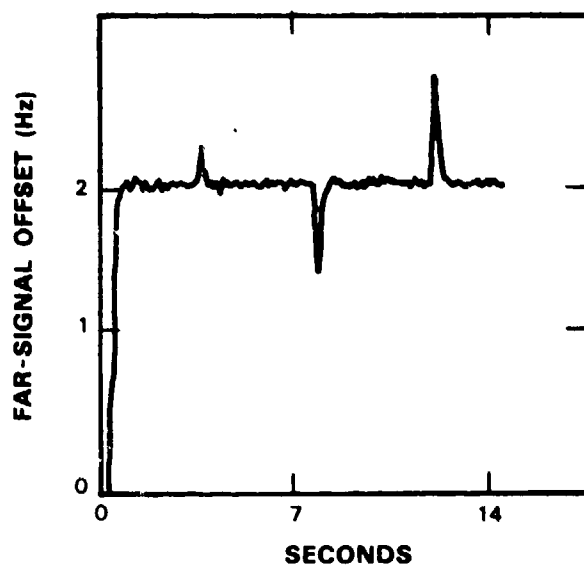
In the next case, the received signal is corrupted by impulse noise—a distortion typically arising from the switching equipment in the telephone system.<sup>3</sup> The impulses have about twice the height of the far-end signal, have a width of one baud, and occur at a rate of 5/s. As shown in Figure 4-5, the system again recovers from these distortions and from the resulting decision errors. The decision error rate in steady-state mode is about 10/s, which is the number expected with the 5/s impulse rate, assuming each impulse affects two DPSK symbols. This same example was also run with a near-echo-to-signal ratio of 30 dB and 40 dB; the 40 dB case is shown in Figure 4-6. Although the system transient responses are not well-understood (due to the complex coupling of five adaptive filters and two phase-locked loops), the steady-state suppression predicted by Equation (3-9) is still approximately achieved.



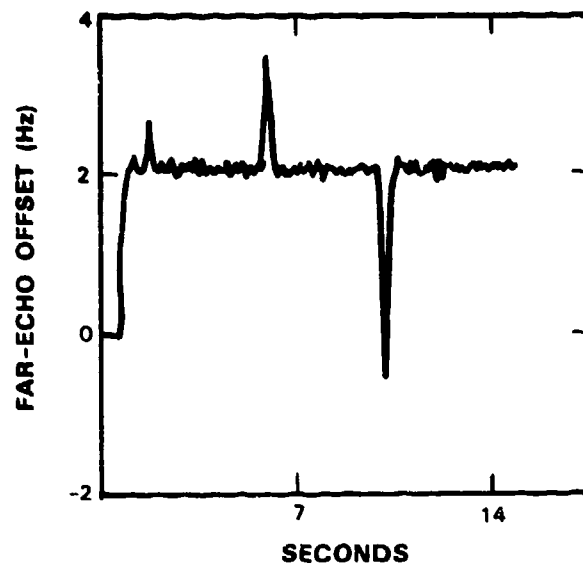
(a)



(b)



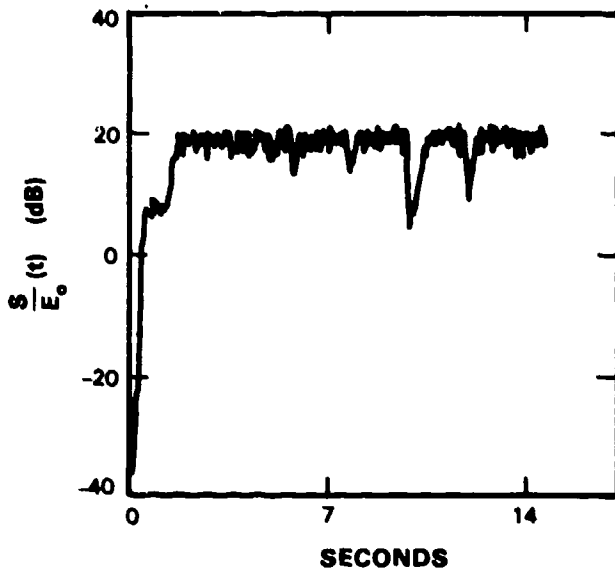
(c)



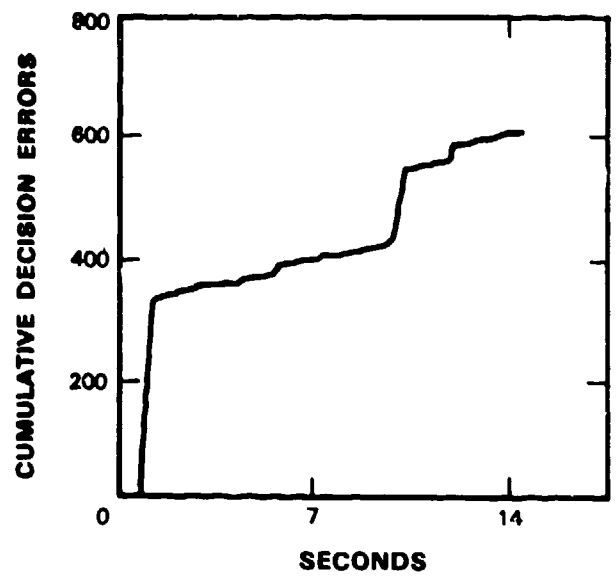
(d)

Figure 4-5. Performance of complete modem with phase hits and impulse noise. (a)  $S/E_0$ , (b) accumulated receiver errors, (c) far-end-signal frequency-offset estimate, (d) far-echo frequency-offset estimate.

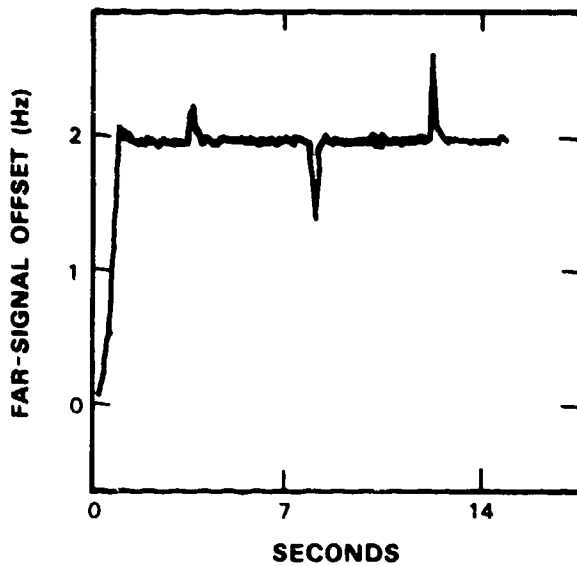
78087-6



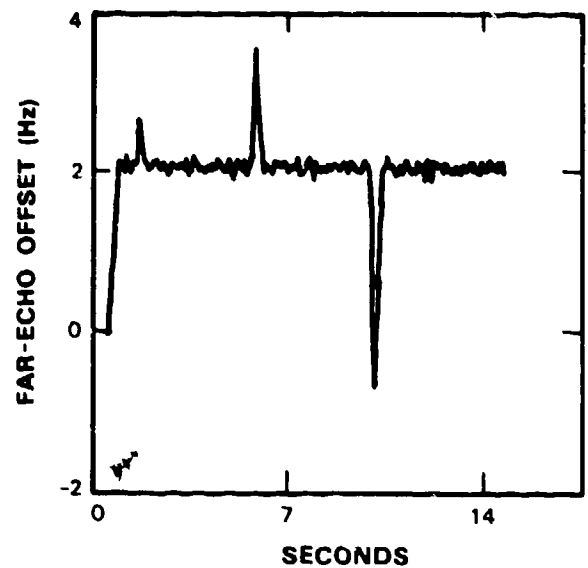
(a)



(b)



(c)



(d)

Figure 4-6. Performance of complete modem design with phase hits and impulse noise (near-echo-to-signal ratio = 40 dB). (a)  $S/E_0$ , (b) accumulated receiver errors, (c) far-end-signal frequency-offset estimate, (d) far-echo frequency-offset estimate.

## 5. AN RLS ADAPTIVE-REFERENCE ECHO-CANCELLING MODEM

We saw earlier in Section 2.3 that the near-echo-cancelling adaptive-reference algorithm, although outperforming the ZREC system, did not have sufficient responsiveness to track a linearly changing phase due to frequency offset. In this section we consider the use of recursive least squares (RLS) as an alternative to LMS. On each iteration the RLS algorithm gives an exact solution<sup>11</sup> to the least-squares cancellation problem based on the observed statistics of the input signal, and thus one would expect faster convergence and more echo suppression than its LMS counterpart. We find, however, similar behavior by the LMS and RLS algorithms. The advantage of the RLS algorithm comes from its ability to modify its adaptation strategy to take advantage of the observed statistics of the input.<sup>16,17</sup> Since the data stream in this application is uncorrelated from symbol to symbol, no advantage results from the more complex algorithm.

We incorporated the RLS algorithm into the simulation of the system in Figure 2-1. Both the LMS canceller and simulator adaptation procedures were replaced by their RLS complex counterparts. The equalizer adaptation remained LMS. The generic complex recursive equations for RLS<sup>11</sup> are given as

$$\underline{e}(nT) = \underline{c}[(n-1)T] + G(nT) \underline{e}(nT) \exp[-j\omega_c nT] \quad (5-1a)$$

$$G(nT) = \frac{P[(n-1)T] \underline{x}^*(nT)}{\underline{x}^H(nT) P[(n-1)T] \underline{x}^*(nT) + \lambda} \quad (5-1b)$$

$$P(nT) = \frac{P[(n-1)T] - G(nT) \underline{x}^H(nT) P[(n-1)T]}{\lambda} \quad (5-1c)$$

where  $\underline{e}(nT)$  is the error residual driving both the canceller and simulator, and  $\lambda$  is the "forgetting factor." The data vector is denoted by  $\underline{x}(nT)$  and the inverse data correlation matrix by  $P(nT)$  of size  $N \times N$  where  $N$  is the filter length. In order to form a fair behavioral comparison of the LMS and RLS systems, the "forgetting factor" must correspond to the same convergence rate (or time constant) characterizing the LMS update algorithm. Although such a relationship does exist for the case of a single adaptive filter,<sup>16,17</sup> the relationship does not hold for the case of two joint adaptive filters in the adaptive-reference algorithm. Nevertheless, with some trial and error we were able to choose an LMS gain factor and an RLS "forgetting factor" which results in about the same convergence rate for the joint adaptation.

It should be emphasized that since we have simply replaced the LMS adaptation for each filter by its RLS counterpart, we have not solved the minimization problem of (2-6); rather, this replacement corresponds to an independent RLS estimation of the canceller and simulator coefficients and ignores the error residual coupling inherent in the minimization of (2-6) and, thus, we expect suboptimal performance. The exact recursive solution, which also has been simulated, requires a coupled iteration of the form (2-8) with matrices twice the size of those in (5-1). Thus, although this exact recursion can be formulated, the computational requirements are overbearing and, furthermore, no improvement in echo suppression was obtained.



A comparison of the two echo-suppression algorithms is illustrated in Figure 5-1. The two RLS filter adaptations are of the form (5-1). The convergence gain for LMS is set at .05 and the "forgetting factor" for RLS is set at .99. The background S/N = 20 dB and all other specifications are the same as in Table II. The LMS residual suppression is about the same as that which resulted from RLS. As indicated earlier this behavior is predictable, since the input to each adaptive filter is uncorrelated from symbol to symbol. It is somewhat surprising that the RLS performs slightly worse; however, the RLS algorithm is known to be sensitive to quantization noise buildup which may explain this behavior.<sup>16</sup> We also tested the RLS tracking ability by introducing a 2-Hz frequency offset in the far-end echo path at 3000 bauds, as in the example of Figure 2-3. The RLS algorithm behaved similarly to LMS, quickly losing suppression at the onset of the frequency offset, then attempting to track the linear phase due to frequency offset by rotation of the complex canceller coefficients. As with LMS, the forgetting factor does not allow fast enough rotation to track the linearly changing phase.

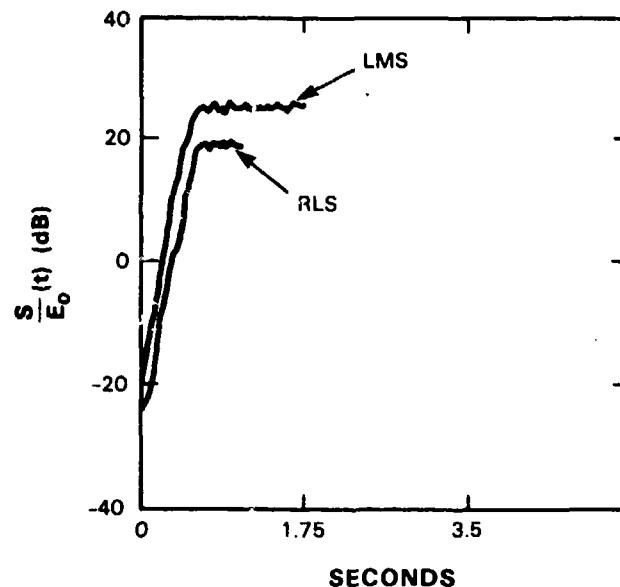


Figure 5-1. Comparison of LMS and RLS near-echo adaptive-reference cancellers.

## 6. IMPLEMENTATION

In this section we explore what it would take to build an echo canceller of this design. We first look at the computational requirements of the algorithm and then show a possible implementation based on the AT&T DSP32 floating-point digital signal processing chip.

The main computational load in the modem design involves five adaptive (complex) filters running simultaneously. Table III illustrates the operations required for each of the adaptive filters. The first component of the computational load is the FIR filter. Each filter is 88 taps long. Since the input and the filter taps for each filter are complex, each filter tap at each time sample requires 4 multiplies. Since the inputs to the echo cancellers and channel simulator consist of data symbols, only every third input is nonzero. Thus, the number of filter operations is roughly 30 per time sample for these filter structures. These filters are updated at the sample rate of 7200 samples/s. The equalizers, operating on the received signal, require 88 filter operations per tap, per sample time. Since decisions associated with each equalizer occur at the baud rate, only 2400 filtering operations per second are required for these filters. As an example of the calculations required to determine the number of multiplies per second found in Table III, consider the near-echo case. Here we are computing 7200 filter outputs per second and for each output; 4 multiplies occur for each of 30 taps, thus yielding 864,000 multiplies per second. The same applies to the near-echo and channel simulator filters. A similar calculation yields the 845,000 multiplies per second for the adaptive filters within each receiver.

TABLE III Computational Requirements For Modem Algorithm					
	Near Echo	Far Echo	Channel Simulator	Signal Receiver	Echc Receiver
<b>Filtering</b>					
Summer Taps	30	30	30	88	88
Rate	7200	7200	7200	2400	2400
Multiplies/Tap	4	4	4	4	4
Multiplies/s	864K	864K	864K	845K	845K
<b>Update</b>					
Update Taps	30	30	30	88	88
Rate	7200	7200	7200	2400	2400
Multiplies/Tap	4	4	4	4	4
Multiplies/s	864K	864K	864K	845K	845K
<b>Total Multiplies/s:</b>	1728K	1728K	1728K	1690K	1690K

The second component of the computational load occurs in the filter update equations. Again, for the cancellers and the simulator, since the input data stream is sparse, only 30 complex multiplies are required per update. Since 7200 vector coefficient updates occur per second, a total of roughly 864,000 multiplies per second are required. Similar calculations yield a total of approximately 845,000 multiplies per second for updating each adaptive filter within the far signal and far-echo receiver structures. The total number of multiplies per second required for each distinct adaptive component is given in the final row of Table III.

The WE DSP32 is capable of processing 32-bit floating-point numbers at a speed of 4 million multiply-add operations per second. Using a floating-point processor for the new modem algorithm has three obvious advantages over more conventional fixed-point processors, such as the Texas Instrument TMS320: (1) the current simulation in 32-bit floating-point arithmetic on the VAX 780 in the high level language "C" need not be simulated in fixed-point — an extremely tedious task — thus, precision will not be a problem; (2) the large dynamic range of floating-point numbers makes it easy to program numerical algorithms where the numbers in intermediate steps of the calculation can change over several orders-of-magnitude; (3) the basic data arithmetic unit (DAU) is multiply and add, and is capable of executing 4 million of these instructions per second — this basic operation is exactly what is required by the echo-cancelling finite-impulse-response filters and filter coefficient-update equations. In addition, the DSP32 has 4 kbytes of random access memory (RAM) and 2 kbytes of internal read only memory (ROM); memory can also be expanded off-chip. Other DSP chips could also be considered. The Analog Devices ADSP2100 is approximately twice as fast as the DSP32 but has only fixed-point arithmetic. It uses 16-point quantities but can maintain 40-bit precision in multiply-accumulate loops. More new announcements of DSP chips are expected in the near future.

The quantities in Table III are well within the range of the limits of the DSP32 chip which can handle 4 million 32-bit multiplies per second. One possible implementation of the modem algorithm, using three DSP32 chips, is depicted in Figure 6-1. The far-echo receiver and far-echo canceller are implemented in the first DSP32. The channel simulator and the far-signal receiver are implemented in the second processor. In fact, these two units are nearly identical in structure, each unit requiring roughly 2.5 million multiply accumulates per second. The remaining computational capability in each unit is used for the phase-locked loop, complex modulations and demodulations, and signal subtractions. The near-echo canceller and transmitter are incorporated in the third DSP chip. Since the pulse shaper is 31 samples long and the sampling rate is 7200 samples/s, a total of roughly  $7200 \times 31 \times 4 = 892,800$  multiply-accumulates/s is required for the transmitter. Thus, the third DSP32 chip will implement a total of roughly 2.6 million multiply-accumulates/s with a remaining capability for other operations such as symbol modulation.

This design is fairly aggressive since the basic inner loop of the computations requires about 65 percent of the processing capability of the chips. Determining whether the remaining code could be run in the available time would take a more detailed study. If it did not, another processor could be added, although the problem would not partition as nicely. Another option

would be to reduce the lengths of some of the filters. This parameter was not examined in detail in this study since it would require testing over a large number of channel characteristics rather than a typical channel which was used in this study

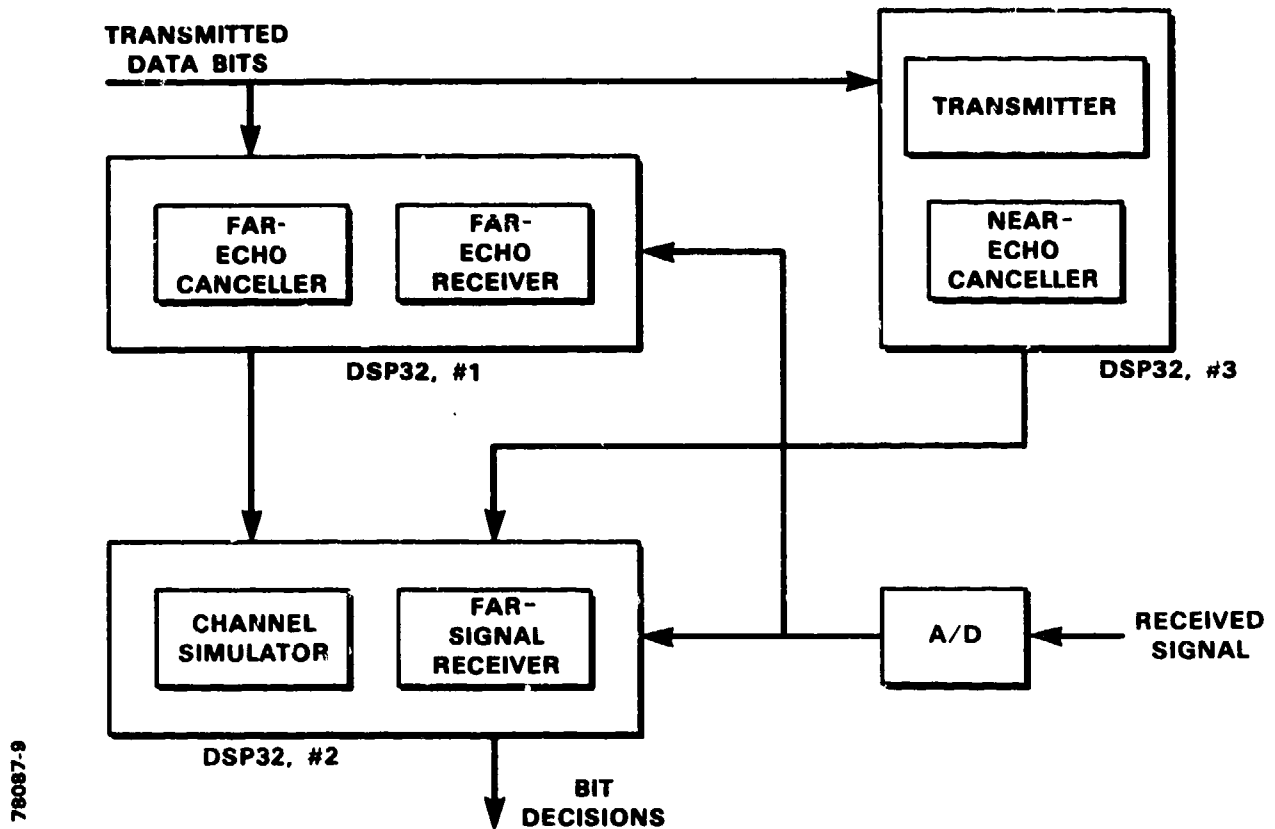


Figure 6-1. DSP32 configuration of the modem design.

## 7. SUMMARY AND DISCUSSION

We have described a full-duplex adaptive (LMS) reference echo-cancelling modem which accounts for both near and far echo. The adaptive-reference technique generates an estimate of the far-end signal which is used to obtain improved estimates of the near and far echos. Estimation of the frequency offset in the far echo uses a separate receiver structure devoted to joint estimation of the near-end transmit symbols and far-echo frequency offset. When simulated at 4800 b/s, this algorithm was demonstrated to be robust for typical white noise background levels. The far-end echo-cancelling modem design also accommodates frequency offset in the far-end signal. The performance of the complete far- and near-echo canceller was simulated, and its steady-state behavior was predicted under a variety of conditions. The algorithm is stable in the presence of typical background white and impulse noise and when the far-end signal and echo are disturbed by phase hits in the carrier. The dynamic behavior awaits analytic study as does the coupling of the iterative update procedures.

A second method for improving the canceller's tracking ability in the presence of frequency offset uses an RLS version of the adaptation process. Here the LMS adaptive canceller and simulator were replaced by their RLS counterparts. Since the input to these filters is white, the RLS adaptation gave no advantage over the LMS. The RLS adaptation may be useful, however, in channel equalization, especially at very high data rates.

Finally, we briefly explored the computational requirements of the adaptive (LMS) near/far-echo-cancelling modem design. A real-time implementation is probably feasible with the use of three floating-point WE DSP32 signal processing chips; however, a more exhaustive design study will be required to refine this preliminary configuration.

A number of important questions still remain. First, we have made no serious attempt to "fine-tune" the echo-cancelling modem algorithm nor to seriously test the system at its limits. In particular, choice of the convergence gains for the adaptive filters and phase-locked loops need more consideration. An exhaustive test of the system in Figure 3-5 should then be made to find just how far we can push the algorithm before breakdown. Additional future research may also include developing a passband version of the (currently baseband) echo-cancelling modem design. With such a system, it may be possible to eliminate many of the computationally burdensome modulators/demodulators. Finally, this system may have additional importance at 9600 b/s. At such a high data rate, however, other distortions may require attention as, for example, phase jitter. It appears that estimating and compensating for such distortions should not pose a problem.

## **ACKNOWLEDGEMENTS**

The authors would like to thank Professor John Proakis, Professor David Messerschmitt, Ronald Cohn, Douglas Rahikka, and Richard Dean for helpful discussions.

## REFERENCES

1. J.J. Werner, AT&T Tech. J. **64**, No. 1, 91 (1985).
2. S.B. Weinstein, IEEE Trans. Commun. **COM-25**, No. 7, 654 (1987).
3. F.P. Duffy and T.W. Thatcher, Bell Sys. Tech. J. **50**, No. 4, 1311 (1971).
4. P.H. Wittke, S.R. Penstone, and R.S. Keightley, IEEE J. Selec. Areas Commun. **SAC-2**, No. 5, 703 (1984).
5. R.D. Gitlin and S.B. Weinstein, IEEE Trans. Commun. **COM-26**, No. 6, 833 (1978).
6. D.D. Falconer, IEEE Trans. Commun. **COM-30**, No. 9, 2083 (1982).
7. K.H. Mueller, IEEE Trans. Commun. **COM-24**, No. 9, 956 (1976).
8. J. Werner, IEEE J. Selec. Areas Commun. **SAC-2**, No. 5, 722 (1984).
9. M.M. Sondhi and D.A. Berkley, Proc. IEEE **68**, No. 8, 948 (1980).
10. B. Widrow and S.D. Stearns, *Adaptive Signal Processing* (Prentice-Hall, Englewood Cliffs, New Jersey, 1985).
11. J.G. Proakis, *Digital Communications* (McGraw-Hill Book Co., New York, New York, 1983).
12. D.D. Falconer, Bell Sys. Tech. J. **55**, No. 3, 317 (1976).
13. D.D. Falconer, Bell Sys. Tech. J. **55**, No. 4, 409 (1976).
14. R.D. Gitlin and J.S. Thompson, IEEE Trans. Commun. **COM-26**, No. 8, 1211 (1978).
15. A.J. Viterbi, *Principles of Coherent Communications*, (McGraw-Hill Book Co., New York, New York, 1966).
16. F. Ling and J.G. Proakis, 1984 Int. Conf. Acoust., Speech Signal Proc., San Diego, California, March 1984, p. 371.
17. E. Eleftheriou and D.D. Falconer, 1985 Int. Conf. Acoust., Speech Signal Proc., Tampa, Florida, March 1985, p. 1145.
18. J.R. Boddie, W.P. Hays, and J. Tow, 1986 Int. Conf. Acoust., Speech Signal Proc., Tokyo, Japan, April 1986, p. 421.

**SECURITY CLASSIFICATION OF THIS PAGE**

A182212

REPORT DOCUMENTATION PAGE				
1a. REPORT SECURITY CLASSIFICATION Unclassified		1b. RESTRICTIVE MARKINGS		
2a. SECURITY CLASSIFICATION AUTHORITY		3. DISTRIBUTION/AVAILABILITY OF REPORT Approved for public release; distribution unlimited.		
2b. DECLASSIFICATION/DOWNGRADING SCHEDULE				
4. PERFORMING ORGANIZATION REPORT NUMBER(S) Technical Report 771		5. MONITORING ORGANIZATION REPORT NUMBER(S) ESD-TR-86-183		
6a. NAME OF PERFORMING ORGANIZATION Lincoln Laboratory, MIT	6b. OFFICE SYMBOL (If applicable)	7a. NAME OF MONITORING ORGANIZATION Electronic Systems Division		
6c. ADDRESS (City, State, and Zip Code) P.O. Box 73 Lexington, MA 02173-0073		7b. ADDRESS (City, State, and Zip Code) Hanscom AFB, MA 01731		
8a. NAME OF FUNDING/SPONSORING ORGANIZATION Department of Defense	8b. OFFICE SYMBOL (If applicable)	9. PROCUREMENT INSTRUMENT IDENTIFICATION NUMBER		
8c. ADDRESS (City, State, and Zip Code) The Pentagon Washington, DC 20301		10. SOURCE OF FUNDING NUMBERS		
		PROGRAM ELEMENT NO. 33401F 64754F	PROJECT NO. 51	TASK NO. WORK UNIT ACCESSION NO.
11. TITLE (Include Security Classification) Adaptive-Reference Near- and Far-Echo Cancellation in the Presence of Frequency Offset				
12. PERSONAL AUTHOR(S) Quatieri, Thomas F. and O'Leary, Gerald C.				
13a. TYPE OF REPORT Technical Report	13b. TIME COVERED FROM _____ TO _____	14. DATE OF REPORT (Year, Month, Day) 1987, May, 22		15. PAGE COUNT 56
16. SUPPLEMENTARY NOTATION None				
17. COSATI CODES			18. SUBJECT TERMS (Continue on reverse if necessary and identify by block number)	
FIELD	GROUP	SUB-GROUP	echo cancellation frequency offset far echo frequency offset full-duplex data transmission	
			adaptive filter far echo least mean squares	
			adaptive reference near echo recursive least squares voiceband	
19. ABSTRACT (Continue on reverse if necessary and identify by block number)  This report presents the results of a study of the applicability of various echo-cancelling techniques to the problem of improving the transmission of data over voiceband telephone channels. The principal result of the study is a design for a novel echo-cancelling configuration which permits the cancellation of a far-echo component containing a frequency offset. The modem design is based on an adaptive-reference echo canceller which has the advantage that interference to the echo canceller caused by the far-end signal can be eliminated by subtracting an estimate of the far-end signal based on receiver decisions. To estimate the frequency offset, the system uses a separate receiver structure for the far echo which provides equalization of the far-echo channel and tracks the frequency offset in the far echo. The feasibility of the echo-cancelling algorithm is demonstrated at 4800 b/s data transmission.				
20. DISTRIBUTION/AVAILABILITY OF ABSTRACT <input type="checkbox"/> UNCLASSIFIED/UNLIMITED <input checked="" type="checkbox"/> SAME AS RPT. <input type="checkbox"/> C USERS		21. ABSTRACT SECURITY CLASSIFICATION Unclassified		
22a. NAME OF RESPONSIBLE INDIVIDUAL Major Thomas J. Alpert, USAF		22b. TELEPHONE (Include Area Code) (617) 863-5500 x2330		22c. OFFICE SYMBOL ESD/TML